



UNIVERSITA' DEGLI STUDI DI MILANO

FACOLTÀ DI MEDICINA E CHIRURGIA

Dottorato in Medicina del Lavoro e Igiene Industriale

CICLO XXVII

**SUSCEPTIBILITY TO PARTICULATE
MATTER AND HEALTH EFFECTS
MEDIATED BY microRNAs CARRIED IN
PLASMA EXTRACELLULAR VESICLES**

Relatore: Chiar.mo Prof. Pier Alberto BERTAZZI

Direttore: Chiar.mo Prof. Giovanni COSTA

Tesi di Dottorato di:

Laura Wanda Pergoli

Matr. N. R09653

Anno Accademico 2013/2014

ABSTRACT	4
INTRODUCTION.....	7
AIR POLLUTION	7
PARTICULATE MATTER.....	11
PM AND CARDIOVASCULAR HEALTH EFFECTS	15
EXTRACELLULAR VESICLES	17
1) Exosomes	18
2) Microvesicles.....	20
BIOGENESIS OF EXTRACELLULAR VESICLES.....	22
miRNAs: BIOGENESIS, MECHANISMS OF ACTION AND ROLES.....	24
BIOLOGICAL AND PATHOLOGICAL ROLES OF EXTRACELLULAR VESICLES	27
SPECIFIC AIMS.....	33
MATERIALS AND METHODS.....	35
STUDY POPULATION	35
EXPOSURE ASSESMENT	37
1) Air Monitoring Stations.....	38
2) FARM Eulerian Model.....	39
WORKFLOW PROCESS	41
EXTRACELLULAR VESICLES ISOLATION.....	41
EVs IMMUNOPHENOTYPING BY FLOW CYTOMETRY	42
EVs COUNT AND SIZE	47
miRNAs EXTRACTION.....	49

miRNAs REVERSE TRANSCRIPTION	51
REAL TIME-PCR.....	53
RESULTS	58
STUDY SUBJECT CHARACTERISTICS.....	58
COMPARISON BETWEEN FARM MODEL AND MONITORING STATION PM ₁₀ LEVELS.....	62
ASSOCIATION BETWEEN PM ₁₀ , EVs AND MVs SUBPOPULATION	65
INTERACTION BETWEEN PM ₁₀ AND OBESITY.....	68
ASSOCIATION BETWEEN miRNAs EXPRESSION AND PM ₁₀ EXPOSURE	70
MEDIATION ANALYSIS TO INVESTIGATE THE ROLE OF miRNAs EXPRESSION AS MEDIATOR OF THE EFFECT OF PM ₁₀ ON CARDIAC OUTCOMES:SYSTOLIC AND DIASTOLIC BLOOD PRESSURE.....	74
PATHWAY ANALYSIS FOR THE CANDIDATE miRNAs.....	78
DISCUSSION.....	79
REFERENCES.....	84

ABSTRACT

Air pollution exposure is a major problem worldwide and has been linked to many diseases. PM₁₀ is one of the components of air pollution and it includes a mixture of compounds.

Several studies suggest that PM produces significant effects on the cardiovascular system, in relation to acute as well as chronic exposure.

This process has been extensively studied, but to date it has not yet been fully understood. Ambient particles have been shown to produce a strong inflammatory reaction, and beside pro-inflammatory mediators, cell-derived membrane Extracellular Vesicles (EVs) are also released. EVs (particularly microvesicles) might be the ideal candidate to mediate the effects of air pollution, since potentially they could transfer miRNAs, after internalization within target cells through surface-expressed ligands, enabling intercellular communication in the body.

Our hypothesis is that, after air pollution exposure, the respiratory system can release extracellular vesicles that could reach the systemic circulation and lead to the development of endothelial dysfunction.

The aim of the study is to determine whether exposure to air particles and PM-associated metals can modify EVs in plasma in term of:

- miRNAs content
- Quantity of MVs subpopulations

Our study population represents a subgroup of the SPHERE projects that includes patients enrolled from Center for Obesity and Weight Control of the Department of Environmental and Occupational Health, University of Milan

and IRCCS Fondazione Ca'Granda – Ospedale Maggiore Policlinico. In particular we recruited 883 overweight/obese subjects for miRNAs study (recruited from 2010 till 2012) and 266 (recruited from January till November 2013) subjects for MVs characterization. We chose overweight/obese people because some evidence shows that obesity may bring greater susceptibility to the adverse cardiovascular effects of PM exposure.

Exposure is defined using a multifaceted approach. In particular, PM₁₀ is assigned to each subjects following two approaches: (1) use of daily PM₁₀ concentration series from air quality monitors; (2) use of daily PM₁₀ concentration estimates by the FARM model (the flexible air quality regional model) supplied by ARPA Lombardy.

In the first part of the study, we analyzed the variation, in term of concentration, of plasma EVs in association with PM₁₀ exposure. In particular we decided to investigate 5 subpopulations of microvesicles (MVs) by flow cytometry (MACS Quant Analyzers-Miltenyi Biotech): MVs from monocytes (CD14+), MVs from platelets (CD61+), MVs from neutrophils (CD66+), MVs from endothelium (CD105+), MVs from epithelium (EpCAM+).

The second phase of the study represents a discovery stage that involves a miRNAs expression profiling using the OpenArray technology (QuantStudio™ 12K FlexOpenArray-Life Technologies).

The results of MVs subpopulation analysis in association with PM₁₀ exposure show an increase of 6.6% in the concentration of MVs CD61+ (from platelets); 3.4% for MVs CD66+ (neutrophils); 3.9% MVs for CD105+ (endothelium); 7% for MVs CD14+ (monocytes); while there is no significant association for MVs

EpCAM+ (from pulmonary epithelium). These results indicate the percentage increase of MVs concentration with an increase of $1\ \mu\text{g} / \text{m}^3$ of PM_{10} . The total concentration of extracellular vesicles was analyzed by Nanoparticle Tracking Analysis (NTA), allowing to separate microvesicles from exosomes. The total amount of microvesicles is associated with PM_{10} exposure, while the total amount of exosomes is not significant.

From miRNAs analysis, performed through TaqMan Open Array Real Time PCR, we test the association between PM_{10} exposure and the different levels of expression of 733 human miRNAs.

This phase of the SPHERE study has the aim of screening the entire miRNome on a population of 833 subjects. From the results of this analysis have emerged 52 miRNAs as strongly associated with PM_{10} exposure. We performed a Mediation Analysis to investigate the potential role of the top 10 miRNAs as mediators of the effect of PM_{10} exposure on cardiac outcomes, as Systolic Blood Pressure and Diastolic Blood Pressure. We can estimate that 36.8% of the effect of PM_{10} on Systolic Blood Pressure is mediated by miR-106a. Interestingly miR-106a seems to play a crucial regulatory role in regulate macrophage inflammatory responses, and is well known that macrophage infiltration is involved in the processes of formation of atherosclerotic plaques.

The identified expression profile may provide a useful starting point for the understanding of the key mechanism that links PM_{10} exposure to the onset of cardiovascular diseases.

INTRODUCTION

AIR POLLUTION

Air pollution exposure is a major problem worldwide and has been linked to many diseases.

Air pollution consists of gas and particle contaminants that are present in the atmosphere. Gaseous pollutants include SO_2 , NO_x , ozone, carbon monoxide (CO), volatile organic compounds (VOCs), certain toxic air pollutants, and some gaseous forms of metals. Particle pollution ($\text{PM}_{2.5}$ and PM_{10}) includes a mixture of compounds. The majority of these compounds can be grouped into five categories: sulfate, nitrate, elemental (black) carbon, organic carbon, and crustal material (Table 1).

Some pollutants are released directly into the atmosphere. These include gases, such as SO_2 , and some particles, such as crustal material and elemental carbon. Other pollutants are formed in the air.

Ground-level ozone forms when emissions of NO_x and VOCs react in the presence of sunlight. Similarly, some particles are formed from other directly emitted pollutants. For example, particle sulfates result from SO_2 and ammonia (NH_3) gases reacting in the atmosphere. Commonly, emissions come from large stationary fuel combustion sources (such as electric utilities and industrial boilers), industrial and other processes (such as metal smelters, petroleum refineries, cement kilns, manufacturing facilities, and solvent utilization), and mobile sources including highway vehicles and non-road

sources (such as recreational and construction equipment, marine vessels, aircraft, and locomotives).

Sources emit different combinations of pollutants. For example, electric utilities release SO_2 , NO_x , and Particles Fossil fuel combustion is the primary source contributing to CO_2 emissions. Major sources of fossil fuel combustion include electricity generation, transportation (including personal and heavy-duty vehicles), industrial processes, residential, and commercial.[1]

Health, Environmental, and Climate Effects of Air Pollution

Pollutant	Health Effects	Environmental and Climate Effects
Ozone (O ₃)	Decreases lung function and causes respiratory symptoms, such as coughing and shortness of breath; aggravates asthma and other lung diseases leading to increased medication use, hospital admissions, emergency department (ED) visits, and premature mortality.	Damages vegetation by visibly injuring leaves, reducing photosynthesis, impairing reproduction and growth, and decreasing crop yields. Ozone damage to plants may alter ecosystem structure, reduce biodiversity, and decrease plant uptake of CO ₂ . Ozone is also a greenhouse gas that contributes to the warming of the atmosphere.
Particulate Matter (PM)	Short-term exposures can aggravate heart or lung diseases leading to symptoms, increased medication use, hospital admissions, ED visits, and premature mortality; long-term exposures can lead to the development of heart or lung disease and premature mortality.	Impairs visibility, adversely affects ecosystem processes, and damages and/or soils structures and property. Variable climate impacts depending on particle type. Most particles are reflective and lead to net cooling, while some (especially black carbon) absorb energy and lead to warming. Other impacts include changing the timing and location of traditional rainfall patterns.
Lead (Pb)	Damages the developing nervous system, resulting in IQ loss and impacts on learning, memory, and behavior in children. Cardiovascular and renal effects in adults and early effects related to anemia.	Harms plants and wildlife, accumulates in soils, and adversely impacts both terrestrial and aquatic systems.
Oxides of Sulfur (SO _x)	Aggravate asthma, leading to wheezing, chest tightness and shortness of breath, increased medication use, hospital admissions, and ED visits; very high levels can cause respiratory symptoms in people without lung disease.	Contributes to the acidification of soil and surface water and mercury methylation in wetland areas. Causes injury to vegetation and local species losses in aquatic and terrestrial systems. Contributes to particle formation with associated environmental effects. Sulfate particles contribute to the cooling of the atmosphere.

Oxides of Nitrogen (NO _x)	Aggravate lung diseases leading to respiratory symptoms, hospital admissions, and ED visits; increase susceptibility to respiratory infection.	Contributes to the acidification and nutrient enrichment (eutrophication, nitrogen saturation) of soil and surface water. Leads to biodiversity losses. Impacts levels of ozone, particles, and methane with associated environmental and climate effects.
Carbon Monoxide (CO)	Reduces the amount of oxygen reaching the body's organs and tissues; aggravates heart disease, resulting in chest pain and other symptoms leading to hospital admissions and ED visits.	Contributes to the formation of CO ₂ and ozone, greenhouse gases that warm the atmosphere.
Ammonia (NH ₃)	Contributes to particle formation with associated health effects.	Contributes to eutrophication of surface water and nitrate contamination of ground water. Contributes to the formation of nitrate and sulfate particles with associated environmental and climate effects.
Volatile Organic Compounds (VOCs)	Some are toxic air pollutants that cause cancer and other serious health problems. Contribute to ozone formation with associated health effects.	Contributes to ozone formation with associated environmental and climate effects. Contributes to the formation of CO ₂ and ozone, greenhouse gases that warm the atmosphere.
Mercury (Hg)	Causes liver, kidney, and brain damage and neurological and developmental damage.	Deposits into rivers, lakes, and oceans where it accumulates in fish, resulting in exposure to humans and wildlife.
Other Toxic Air Pollutants	Cause cancer; immune system damage; and neurological, reproductive, developmental, respiratory, and other health problems. Some toxic air pollutants contribute to ozone and particle pollution with associated health effects.	Harmful to wildlife and livestock. Some toxic air pollutants accumulate in the food chain. Some toxic air pollutants contribute to ozone and particle pollution with associated environmental and climate effects.

Table 1. Health, Environmental, and Climate Effects of Air Pollution Components. *U.S Environmental Protection Agency's Report 2010*

PARTICULATE MATTER

PM is a mixture of suspended particles that vary in chemical composition and size.

Particulate matter varies in number, size, shape, surface area, chemical composition and characteristics, and can be of both natural and anthropological origin.

The size distribution of urban ambient particle pollution is usually characterized by aerodynamic diameter (AED) which is defined as the diameter of a sphere of unit density (1g/cm^3) that has the same inertial properties in the gas as the particle of interest.

The size distribution of suspended particles in the atmosphere is tri-modal and includes coarse particles, fine particles, and ultrafine particles.

Coarse particles ($\text{PM}_{2.5-10}$: often defined as those with an aerodynamic diameter $> 2.5\mu\text{m}$) are primarily produced by natural mechanisms such as grinding and wind, and derive mainly from soil and other crustal materials.

Fine particles ($\text{PM}_{2.5}$: diameter $< 2.5 \mu\text{m}$) are derived chiefly from combustion processes. In the urban environment these processes are associated with transportation, manufacturing, and power generation. Ultrafine particles are often defined as particles less than or equal to $0.1 \mu\text{m}$. (Figure 1)

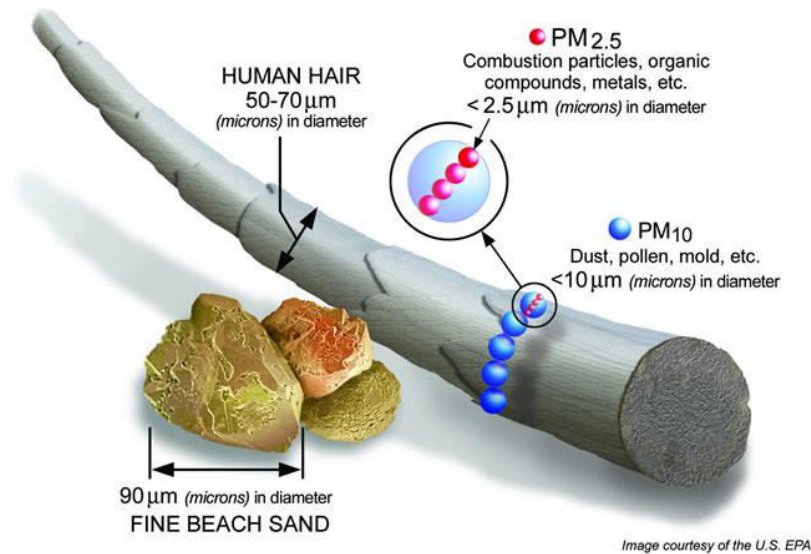


Figure 1. Particle pollution size. U.S EPA

Particles can either be directly emitted into the air (primary PM) or be formed in the atmosphere from gaseous precursors such as sulfur dioxide, oxides of nitrogen, ammonia and non-methane volatile organic compounds (secondary particles).

Primary PM and the precursor gases can have both man-made (anthropogenic) and natural (non-anthropogenic) sources. Anthropogenic sources include combustion engines (both diesel and petrol), solid-fuel (coal, lignite, heavy oil and biomass) combustion for energy production in households and industry, other industrial activities (building, mining, manufacture of cement, ceramic and bricks, and smelting), and erosion of the pavement by road traffic and abrasion of brakes and tyres.

Agriculture is the main source of ammonium.

Secondary particles are formed in the air through chemical reactions of gaseous pollutants.

They are products of atmospheric transformation of nitrogen oxides (mainly emitted by traffic and some industrial processes) and sulfur dioxide resulting from the combustion of sulfur-containing fuels. Secondary particles are mostly found in fine PM.

Soil and dust re-suspension is also a contributing source of PM, particularly in arid areas or during episodes of long-range transport of dust, for example from the Sahara to southern Europe.[2]

PM₁₀ and PM_{2.5} include inhalable particles that are small enough to penetrate the thoracic region of the respiratory system. The health effects of inhalable PM are well documented.

They are due to exposure over both the short term (hours, days) and long term (months, years) and include:

- respiratory and cardiovascular morbidity, such as aggravation of asthma, respiratory symptoms and an increase in hospital admissions;
- mortality from cardiovascular and respiratory diseases and from lung cancer.

There is good evidence of the effects of short-term exposure to PM₁₀ on respiratory health, but for mortality, and especially as a consequence of long-term exposure, PM_{2.5} is a stronger risk factor than the coarse part of PM₁₀ (particles in the 2.5–10 µm range). All-cause daily mortality is estimated to increase by 0.2–0.6% per 10 µg/m³ of PM₁₀[3, 4]. Long-term exposure to PM_{2.5} is associated with an increase in the long-term risk of cardiopulmonary mortality by 6–13% per 10 µg/m³ of PM_{2.5} [5-7]

Susceptible groups with pre-existing lung or heart disease, as well as elderly people and children, are particularly vulnerable. For example, exposure to PM affects lung development in children, including reversible deficits in lung function as well as chronically reduced lung growth rate and a deficit in long-term lung function [8]. There is no evidence of a safe level of exposure or a threshold below which no adverse health effects occur. The exposure is ubiquitous and involuntary, increasing the significance of this determinant of health.

At present, at the population level, there is not enough evidence to identify differences in the effects of particles with different chemical compositions or emanating from various sources. It should be noted, however, that the evidence for the hazardous nature of combustion-related PM (from both mobile and stationary sources) is more consistent than that for PM from other sources [9]. The black carbon part of PM_{2.5}, which results from incomplete combustion, has attracted the attention of the air quality community owing to the evidence for its contribution to detrimental effects on health as well as on climate.

Many components of PM attached to black carbon are currently seen as responsible for health effects, for instance organics such as PAHs that are known carcinogens and directly toxic to the cells, as well as metals and inorganic salts.

PM AND CARDIOVASCULAR HEALTH EFFECTS

Several studies suggest that PM produces significant effects on the cardiovascular system[10-12]. Research on this topic has focused on both the long-term effects of chronic PM exposure and the acute effects of increases in ambient PM on cardiovascular mortality.

In a previous analysis[13], it was shown that for any increase in mortality caused by PM, two thirds of the effect was accounted for by the cardiovascular diseases.

Animal studies show a link between chronic PM exposure and the development of atherosclerosis via systemic inflammation[14, 15]. Human studies show that the effects seem to be mediated by the inflammatory cytokines IL-6, TNF- α , and C reactive protein (CRP). Increases in both IL-6[16] and CRP[17] have been associated with the development of acute myocardial infarction. Ruckerl et al.[18] described transient IL-6 and TNF- α elevations in diabetic patients for 2 days following PM₁₀ exposure. In a prospective cohort study of German patients, Hoffman et al.[19] associated exposure to PM_{2.5} with elevations in CRP.

Other researchers demonstrated similar increases in CRP from PM₁₀ exposure from both combustion[20] and organic matter[21].

Acute exposure to PM causes changes in coagulation and platelet activation providing a more proximal link between PM and coronary artery disease. Many experts consider fibrinogen to be an important risk factor for cardiovascular disease[13]. Ruckerl et al. [18] associated a 5-day cumulative exposure to PM₁₀ with increased fibrinogen levels in survivors of myocardial infarction.

Other pro-coagulant factors, such as plasminogen activator fibrinogen inhibitor-1 (PAI-1), were also associated with PM elevations[21]. Intratracheal instillation of diesel exhaust particles led to increased platelet activation in hamsters and rapid thrombosis formation [22].

Schicker et al.[21] showed that transient increases in PM₁₀ exposure caused during hay-stacking increased platelet aggregation within 2 h of the activity. This activity also increased VonWillebrand factor and Factor VIII, markers of vascular endothelial activation.

The “Harvard Six Cities study,” [11] a cohort study published in 1993, followed 8,111 patients for 16–18 years and showed a 29% (95% CI, 8–47%) increase in the adjusted mortality rate for the most polluted of the cities compared to the least polluted.

Particulate air pollution was positively associated with death from lung cancer and cardiopulmonary disease.

Pope et al. [10] followed this in 1995 with another prospective cohort study of 552,000 patients in 151 metropolitan areas using the American Cancer Society's Cancer Prevention 2 database. These data showed a 17% (95% CI, 9–26%) increase in all-cause mortality and a 31% (95% CI, 17–46%) increase in cardiopulmonary mortality when comparing the most and least polluted cities.

Their research demonstrated an average increase in cardiopulmonary mortality of 9% (95% CI, 3–16%) for each 10- $\mu\text{g}/\text{m}^3$ increase in PM_{2.5}. Subsequently, they determined that a 10 $\mu\text{g}/\text{m}^3$ increase in PM increased ischemic cardiovascular disease mortality by 18% (95% CI, 14–23%) and

mortality from arrhythmia, congestive heart failure, and cardiac arrest by 13% (95% CI, 5–21%).

EXTRACELLULAR VESICLES

Intercellular communication is an essential hallmark of multicellular organisms and can be mediated through direct cell–cell contact or transfer of secreted molecules. In the last two decades, a third mechanism for intercellular communication has emerged that involves intercellular transfer of extracellular vesicles (EVs). The release of apoptotic bodies during apoptosis has been long known[23], but only recently the fact that also healthy cells shed vesicles from their plasma membrane become acknowledged.

The term exosome was initially used for vesicles ranging from 40 to 1,000 nm that are released by a variety of cultured cells[24], but the subcellular origin of these vesicles was unclear. Later, this nomenclature was adopted for 40–100 nm vesicles released during reticulocyte differentiation as a consequence of multivesicular endosome (MVE) fusion with the plasma membrane[25]. However, circulating vesicles are composed of both exosomes and microvesicles (MVs) (Figure 2).

Microvesicles are larger than exosomes (100-1000 nm) and are released into the extracellular space by outward budding of the cell membrane. On the other hand, exosomes are produced by a more complex inward budding of endosomes[26].

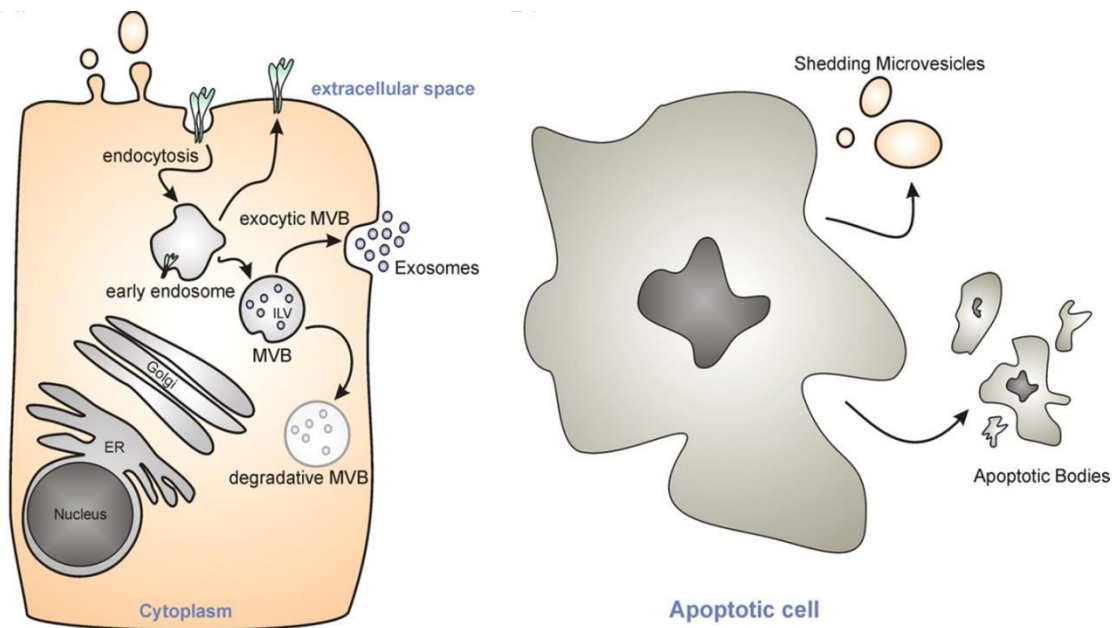


Figure 2. Extracellular vesicles. Meckes D G , and Raab-Traub N J. *Viol.* 2011;85:12844-12854

1) Exosomes

Exosome is the vesicle type that has been studied most intensely.

Exosomes are secreted by many cell types, and have been isolated from several physiological fluids such as sperm[27], urine[28], plasma[29], and bronchial lavage fluid[30]. Their diameter range from 40 to 100 nm, a homogeneous shape, with a density of 1.13-1.19 g/mL in sucrose, and can be sedimented at 100,000 g.

They originate from inward budding of the limiting membrane of multivesicular bodies, which are late endosomal compartments present in the cytosol of the cell. When the multivesicular bodies fuse with the plasma membrane they release exosomes to the extracellular space.

The biogenesis of the exosomes causes the orientation of the membrane proteins to be similar to that of the plasma membrane.

The exosomal membrane is enriched in cholesterol, ceramide, and sphingomyelin and exposes the phospholipid phosphatidylserine.

These markers are not ubiquitously expressed on all exosomes but are found in a large proportion of these vesicles. Therefore, they are generally accepted as exosomal markers. These markers include TSG101, Alix, and the tetraspanins CD9, CD63, and CD81.[31]

They are formed from multivesicular bodies (MVBs), which are intracellular endosomal organelles, characterized by multiple intraluminal vesicles enclosed within a single outer membrane. MVBs are formed from early endosomes, which as prelysosomal structures belong to the degradative endosomal pathway of internalized proteins. They are now known to be involved in numerous endocytic and trafficking functions, including protein sorting, recycling, transport, storage, and release.

There are two types of MVBs, one in the degradative pathway and another in the exocytosis or recycling pathway [32].

Early endosomes can interact with the Golgi apparatus and the endoplasmic reticulum. Exosomes can be formed by endocytosis of the early endosome membrane, having a unique orientation of the invaginated cytoplasmic side[33, 34]. Generation of MVBs as well as secretion of exosomes are mediated by endosomal complexes required for transport (ESCRT complexes). These protein complexes are involved in the recognition of ubiquitinated content by MVBs, as well as the invagination of the MVB outer membrane[35, 36].

The origin of exosomes suggests that their production is stimulated in response to alterations in the microenvironment.

The formation of early endosomes and MVBs has been shown to increase upon signaling via growth factor receptors, suggesting that the cell adjusts exosome production according to its need[28, 37].

2) Microvesicles

Microvesicles are extracellular vesicles ranging in size from 100-1000 nm, with different shapes. Although some authors use the term microvesicles for extracellular vesicles in general, the main differences between exosomes and microvesicles depend on size, formation, and the secretion process. They are formed by regulated release of outward budding of the plasma membrane, consequently they also express antigenic markers of the cell from which they originate.

Several authors use different markers for microvesicles like flotillin-2, selectins, integrins, metalloproteinases, and a high level of phosphatidylserine on the outer surface. There are some resemblances between microvesicles and exosomes: both carry proteins, mRNA, and microRNA (miRNA) and are involved in cellular communication[38, 39], possibly through the horizontal transfer of genetic material, directly stimulating the target cell by transferring receptors or proteins.

The generation of MVs is dependent on both the cell and the stimulus, with lipid bilayer rearrangement (or derangement) being a critical component of MV formation[40]. Main differences between extracellular vesicles are summarized in Table 2.

Vesicle types	Characteristics			
	Origin	Size	Markers	Contents
Exosomes	Endolysosomal pathway; intra-luminal budding of multivesicular bodies and fusion of multivesicular body with cell membrane	40–120 nm	Tetraspanins (such as TSPAN29 and TSPAN30), ESCRT components, PDCD6IP, TSG101, flotillin, MFGE8	mRNA, microRNA (miRNA) and other non-coding RNAs; cytoplasmic and membrane proteins including receptors and major histocompatibility complex (MHC) molecules
Microvesicles	Cell surface; outward budding of cell membrane	50–1,000 nm	Integrins, selectins, CD40 ligand	mRNA, miRNA, non-coding RNAs, cytoplasmic proteins and membrane proteins, including receptors
Apoptotic bodies	Cell surface; outward blebbing of apoptotic cell membrane	500–2,000 nm	Extensive amounts of phosphatidylserine	Nuclear fractions, cell organelles

Table 2. Main differences between extracellular vesicles

BIOGENESIS OF EXTRACELLULAR VESICLES

Exosomes are presumed to be a homogeneous population of vesicles of endocytic origin that are formed by the inward budding of the multivesicular body (MVB) membrane. Cargo sorting into exosomes involves the endosomal sorting complex required for transport (ESCRT) and other associated proteins such as programmed cell death 6 interacting protein (PDCD6IP; also known as ALIX) and tumour susceptibility gene 101 protein (TSG101)[41-43]. In addition to ESCRT, which recognizes ubiquitylated proteins, other ESCRT-independent mechanisms operate to generate exosomes of certain biochemical compositions. For example, in some cells, exosome production requires the lipid ceramide and neutral sphingomyelinase — the enzyme that converts sphingomyelin to ceramide.

Exosomes are secreted following the fusion of MVBs with the cell membrane — a process that is, in some cells, dependent on small GTPases such as RAB27A, RAB11 and RAB31.

An alternative mechanism for the secretion of WNT-bound exosomes was recently shown to involve the SNARE (soluble NSF (N-ethylmaleimide-sensitive factor) attachment protein (SNAP) receptor) protein YKT6. Exosomes display the same membrane orientation as the cell of origin, similarly to microvesicles. Microvesicles, however, represent a relatively heterogeneous population of vesicles that are formed by the outward budding and fission of the cell membrane, which could be controlled by membrane lipid microdomains and regulatory proteins such as ADP-ribosylation factor 6 (ARF6)[44]. Extracellular vesicles can be regarded as signalosomes for

several biological processes. They can be involved in antigen presentation and in the transfer of both major histocompatibility complex (MHC) molecules and antigens, thereby participating in immune regulation. Extracellular vesicles can directly activate cell surface receptors via protein and bioactive lipid ligands, transfer cell surface receptors or deliver effectors including transcription factors, oncogenes and infectious particles into recipient cells⁵. In addition, various RNA species including mRNAs and small regulatory RNAs (for example, microRNAs (miRNAs) and non-coding RNAs) are contained in extracellular vesicles and functionally delivered to recipient cells^[45] (Figure 3).

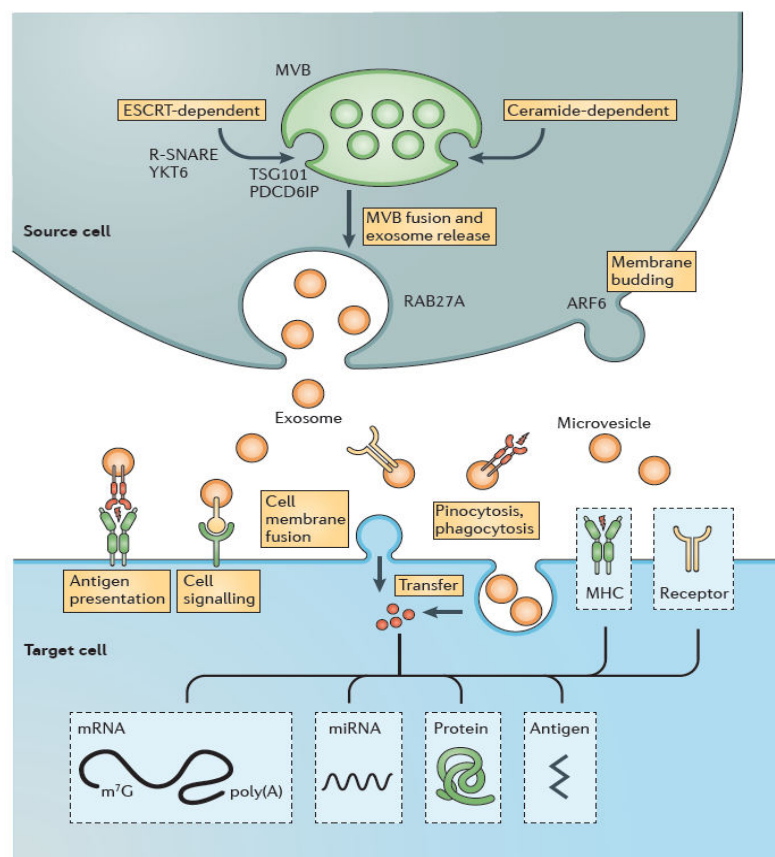


Figure 3: EVs Biogenesis and interactions. Mager, I., Breakefield, X. O., & Wood, M. J. (2013) *Nat Rev Drug Discov*, 12(5), 347-357

miRNAs: BIOGENESIS, MECHANISMS OF ACTION AND ROLES

MicroRNAs, also called miRNAs, are small 19 – 22 nucleotide (nt) sequences of noncoding RNA that work as endogenous epigenetic gene expression regulators.

MicroRNAs are transcribed by RNA polymerase II and/or RNA polymerase III as long 100 – 1000 nt primary, or pri-miRNAs, which are usually capped at the 5' end and are polyadenylated at the 3' end.

Pri-miRNAs are sequentially processed by the ribonucleases Drosha and Pasha (DGCR8) to produce 60–70 nt pre-miRNAs, which have a 5-phosphate and a 2 nt overhang at the 3' end. These products are then exported to the cytoplasm by Exportin-5 where they bind to the ribonuclease Dicer and are processed to yield a double-strand miRNA: miRNA. Finally, a helicase unwinds the duplex into mature miRNAs.[46]

Mature miRNAs are incorporated to the RNA-induced silencing complex (RISC) and bind to the complementary 3'-UTR of their specific target mRNAs.

This either results in inhibition of mRNA translation or promotes its degradation and leads to posttranscriptional gene silencing (PTGS).[47, 48]

Additionally, the RNA-induced transcriptional silencing (RITS) complex, which uses Ago1 instead of Ago2 in its effector complex, was described almost a decade ago.[49]

This complex exerts DNA/histone modifications (e.g., methylation) on the genome and therefore triggers transcriptional gene silencing. Although RITS has been identified in many species so far, it is yet to be confirmed in humans.

In most cases, the “ seed region” (the 7–8 bases after the first or second base of the 5´end of the miRNA) perfectly complements the corresponding target-mRNA sequence.

Nucleotide base pairing also occurs at the 3´region of the miRNA, although it is thought to be weaker and less important than the 5´pairing. Duplex mismatches between miRNA: miRNAs cause the formation of bulge structures in the central region, which may be useful for mRNA regulation (Figure.4).

Because of the short recognition elements, the same miRNA can recognize hundreds of gene targets, , and at the same time, each gene can be targeted by several miRNAs.

MicroRNAs are expressed in all tissues and regulate a wide spectrum of processes, such as cellular differentiation, proliferation, and apoptosis.[50] Moreover, the roles exerted by miRNAs can be very different from each other. For example, in cancer, several miRNAs have been thoroughly characterized and classified as oncogene regulators (oncomiRs); in contrast, others have been described as tumor suppressors, such as the let-7 family which can target oncogenes such as RAS, MYC, HMGA2, and cell cycle checkpoints[46]..

These molecules are not only present in tissues but also in a variety of biologic samples (e.g., whole blood, serum, plasma, urine, and saliva).

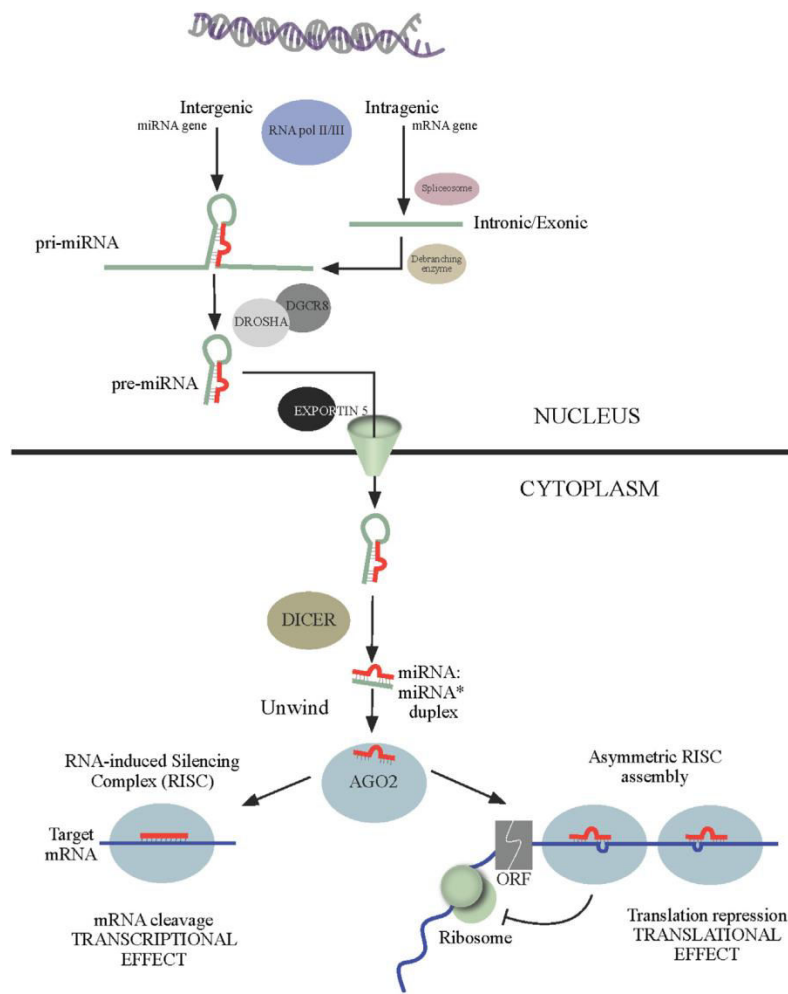


Figure 4. MicroRNA biogenesis and mechanisms of action. *Moreno-Moya, J. M., Vilella, F., & Simon, C. (2014) Fertil Steril, 101(6), 1516-1523.*

BIOLOGICAL AND PATHOLOGICAL ROLES OF EXTRACELLULAR VESICLES

It is now recognized that MVs are an integral part of the intercellular microenvironment and may act as regulators of cell-to-cell communication.

This concept is based on the observation that MVs released from a given cell type may interact through specific receptor ligands with other cells, leading to target cell stimulation directly or by transferring surface receptors.[51, 52]

This implicates that MVs interact only with target cells that specifically recognize rather than just with any cell present in the microenvironment.[53]

This interaction may either be limited to a receptor-mediated binding to the surface of target cells forming a platform for assembly of multimolecular complexes or leading to cell signaling, either to be followed by internalization as a result of direct fusion or endocytic uptake by target cells. Once internalized, MVs can fuse their membranes with those of endosomes, thus leading to a horizontal transfer of their content in the cytosol of target cells.

Extracellular vesicles exert their effects on fundamental biological directly activating cell surface receptors via protein and bioactive lipid ligands and delivering effectors including transcription factors, oncogenes, small and large non-coding regulatory RNAs (such as microRNAs (miRNAs)), mRNAs and infectious particles into recipient cells.[45, 54, 55] Alternatively, they may remain segregated within endosomes and be transferred to lysosomes or dismissed by the cells following the fusion with the plasmamembrane, thus leading to a process of transcytosis[56].

In this way, extracellular vesicles participate in the maintenance of normal physiology — for example, stem cell maintenance[57], tissue repair[58], immune surveillance[59] and blood coagulation[60]. Extracellular vesicles can thus be regarded as signalosomes: multifunctional signalling complexes for controlling fundamental cellular and biological functions.

For example, in the regulation of immune responses, depending on the status of particular immune cells, extracellular vesicles might trigger adaptive immune responses or suppress inflammation in a tolerogenic manner. Extracellular vesicles have been shown to confer immune suppression by several mechanisms: they can enhance the function of regulatory T cells[61], suppress natural killer (NK) and CD8⁺ cell activity[62], and inhibit monocyte differentiation into DCs[63] as well as DC maturation. By contrast, the effects of immune activation can be mediated by extracellular vesicle-promoted proliferation and survival of haematopoietic stem cells and the activation of monocytes[64], B cells[65] and NK cells[66].

In the brain, in addition to classical synaptic neurotransmission, neurons communicate via the secretion of extracellular vesicles that can contribute to a range of neurobiological functions (including synaptic plasticity) — for example, via the increased release of extracellular vesicles containing neurotransmitter receptors from cortical neurons following enhanced glutamatergic activity[67]. Extracellular vesicles have also been implicated in cell phenotype modulation — for example, in converting the haematopoietic stem cell phenotype into a liver cell phenotype and in shifting the bone marrow cell transcriptome and proteome towards a lung phenotype *in vivo*[68]. Importantly,

several reports have implicated extracellular vesicles in stem cell maintenance and plasticity, indicating that stem cell-derived extracellular vesicles have a pivotal role in tissue regeneration following injury[57].

Such wide-ranging cellular and biological functions indicate that extracellular vesicles, by virtue of their pleiotropic signalling effects, may have innate therapeutic potential — for example, in the fields of regenerative medicine and immunotherapy.

Given their fundamental role in regulating biological processes, it is not surprising that in some contexts extracellular vesicles have an important role in disease pathogenesis. The best understood role of extracellular vesicles in disease is their role in tumour biology: numerous studies have implicated extracellular vesicles in driving the formation of a pre-metastatic tumour niche[69]. Extracellular vesicles are capable of stimulating tumor progression[55, 69] via their ability to carry out the following processes: inducing proliferation in cells, thereby directly stimulating tumor growth[39, 70]; stimulating angiogenesis[71]; promoting matrix remodelling via the secretion of matrix proteases[72]; inducing metastasis; and promoting immune escape by modulating T cell activity[73, 74].

Beyond cancer, extracellular vesicles have been implicated in the spread of numerous pathogens, including: HIV-1, via the horizontal transfer of CC chemokine receptor 5 (CCR5), which is used for viral cell entry[75]; Epstein–Barr virus (EBV), via the transfer of viral miRNAs that repress the expression of EBV target genes in non-infected cells[76]; and prions, via the selective delivery of PrP with certain modifications and glycoforms into neuronal cells.

It is also likely that extracellular vesicles contribute to the local propagation of neurodegenerative disease. Neurons are known to communicate through the secretion of extracellular vesicles, which contribute to local synaptic plasticity, but these extracellular vesicles also allow longer-range communication within the central nervous system and have an influence on static neuronal networks located at a distance[77]. This has been elegantly demonstrated in the context of Alzheimer's disease, in which amyloid- β peptides, the toxic protein species for this disease, have been shown to be released in association with exosomes, contributing to pathogenic amyloid- β deposition in other parts of the brain[78]. Similarly, α -synuclein protein has been detected within extracellular vesicles, which could provide a mechanism for the local propagation of Parkinson's disease from enteric neurons to the brainstem and higher cortical centres[79]. Study into the pathological role of EV-mediated miRNA transfer, and their potential application as disease biomarkers or even therapeutic agents, is a field of interest and many potential targets have been identified (Table 3).

Disease	EV source	miRNA content	Putative effect/target	Reference
Asthma	Bronchoalveolar lavage fluid	let-7 and miR-200 families	Biomarkers of mild nonsymptomatic asthma	Levanen et al.[80]
Cardiovascular disease	Injured/dying cardiomyocytes	miR-133a	Biomarker; regulation of cardiac hypertrophy	Kuwabara et al. [81]
	Urine	miR-4516, miR-3183, (miR-3940-5p),(miR-4649-5p)	Biomarkers of salt sensitivity or inverse salt sensitivity index	Gildea et al. [82]
	Plasma of atherosclerosis patients	miR-150	Reduced c-Myb expression and increased cell migration in recipient microvascular endothelial cells	Zhang et al. [83]
Colorectal cancer	Serum of colorectal cancer patients	let-7a, miR-1229, miR-1246, miR-150,miR-21, miR-223, and miR-23a	Biomarkers	Ogata-Kawata et [84]
	Plasma of mice with colorectal cancer xenografts	miR-92a	Enhanced proliferation and motility in recipient endothelial cells, down-regulation of target Dickkopf-3 tumor suppressive gene	Yamada et al.[85]
Lung cancer	Plasma from NSCLC patients	(let-7f), (miR-20b), (miR-30e-3)	NSCLC diagnosis and prognosis	Silva et al. [86]
	Plasma from lung SCC patients	miR-205, miR-19a, miR-19b,miR 30b,miR-20a	SCC biomarkers; oncomiRs	Aushev et al. [87]
Cancer (angiogenesis/ metastasis)	Hypoxic K562 leukaemia cell lines	miR-210	Induction of angiogenesis in recipient endothelial cells	Tadokoro et al.[88]
	Brain metastatic cancer cell lines	miR-210, (miR-19a), (miR-29c)	Biomarkers; potential prognostic agent for brain metastatic breast cancer and melanoma	Camacho et al.[89]
	Metastatic rat adenocarcinoma	miR-494, miR-542-3p	Downregulation of cadhedrin-17 and concomitant up-regulation of matrix metalloproteinase transcription, preparation of a pre-metastatic niche	Rana et al[90]

Stroke	MSCs	miR-133b	Enhanced neurite remodelling; Increased functional recovery and neurovascular plasticity in rat stroke models	Xin et al.[91]
Atherosclerosis	KLF2-transduced or shearstressed HUVECs	miR-143/145 cluster	Regulation of smooth muscle cell function, reduced atherosclerotic lesion formation	Hergenreider et al. [92]

Table 3. miRNAs identified in EVs as relevant to pathophysiological conditions or putative therapeutic applications.

SPECIFIC AIMS

Although several studies have tried to identify the mechanism responsible for the link between PM and cardiovascular diseases, until now this process is not really understood.

The main proposal of our research is to determine whether exposure to PM can modify extracellular vesicles, in particular MVs, in term of quantity, cellular origin and miRNAs content.

Our hypothesis is that, after air pollution exposure, the respiratory system can release extracellular vesicles that could reach the systemic circulation and lead to the development of endothelial disfunctions (Figure 5).

EVs, after internalization within target cells through surface-expressed ligands, may transfer miRNAs enabling intercellular communication in the body.

According to this hypothesis our research will focus on:

Determine whether exposure to air particles and PM-associated metals can modify EVs in plasma in term of:

- miRNAs content
- Quantity of MVs subpopulations

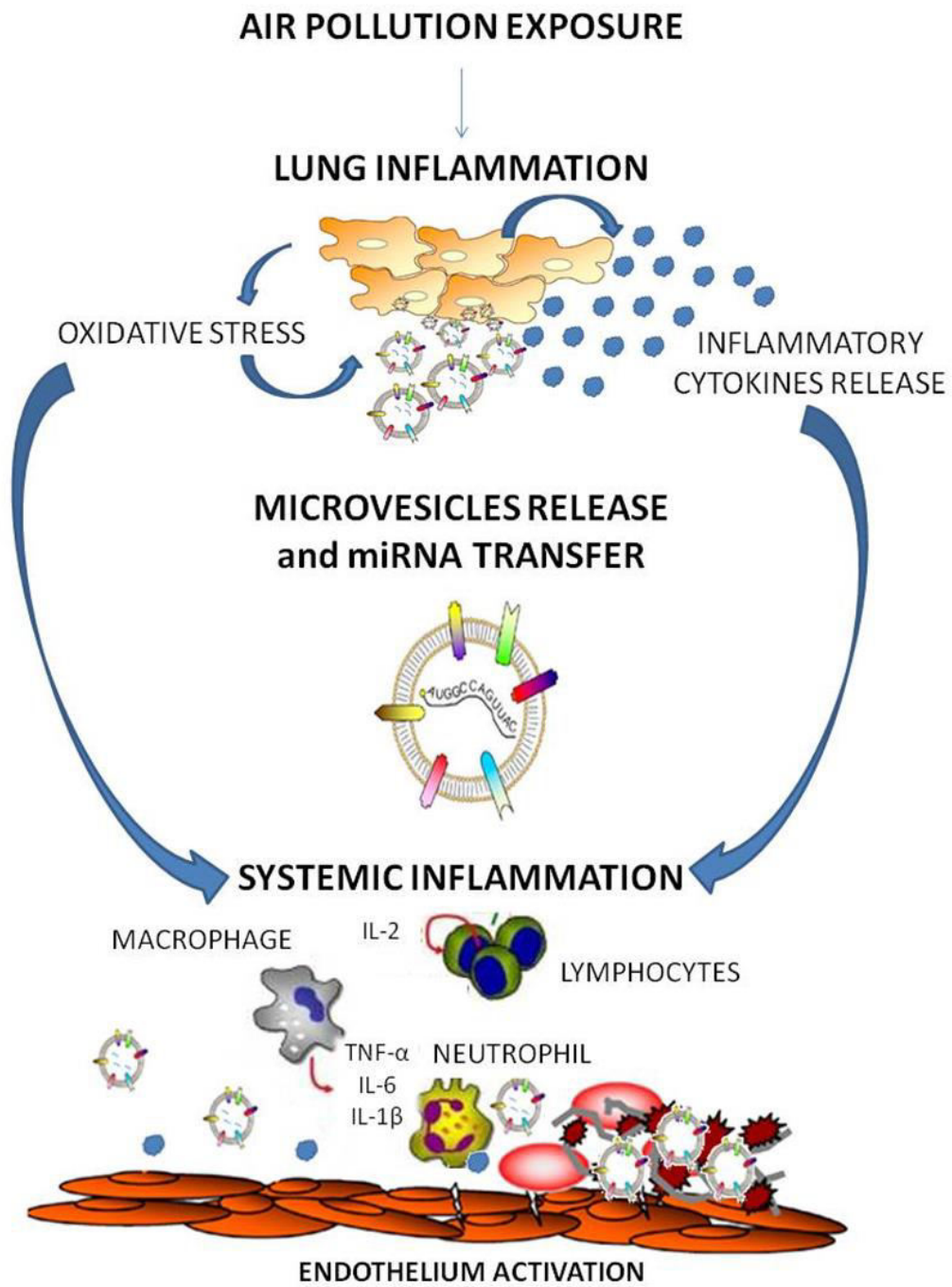


Figure 5. Proposed mechanism for air pollution effects on microvesicle release and cell-to-cell communication.

MATERIALS AND METHODS

STUDY POPULATION

The study population represents a subgroup of the SPHERE project (Susceptibility to Particle Health Effects, miRNAs and Exosomes). The SPHERE study is a cross-sectional study investigating the effects of particulate air pollution on a population of susceptible overweight/obese subjects, recruited in Lombardy Region, Italy. The population examined in this study includes 1250 subjects. The overall study enrollment target will be to recruit 2,000 participants.

We recruited patients from Center for Obesity and Weight Control of the Department of Environmental and Occupational Health, University of Milan and IRCCS Fondazione Ca'Granda – Ospedale Maggiore Policlinico.

We chose obese people because some evidence shows that obesity may bring greater susceptibility [93, 94] to the adverse cardiovascular effects of PM exposure. In addition, It has been shown that obese people are more susceptible to the effect of inflammation in the short-term exposure to PM, presenting higher levels of C-reactive protein and interleukin-6, compared with normal-weight subjects, at the same exposure of PM level [95].

The eligibility criteria for participants are as follows: 1) older than 18 years at enrollment; 2) obese/overweight according to the following definition: overweight is defined as a BMI between 25 and 30 kg/cm², obesity is defined as a BMI of 30 kg/cm² or more; 4) domiciled in Lombardy at the time of the recruitment; 5) agreement to sign an informed consent and donate a blood

sample.

Exclusion criteria include: experienced previously diagnosed cancer, heart disease or stroke in the last year or other chronic diseases such as multiple sclerosis, Alzheimer's disease, Parkinson's disease, depression, bipolar disorder, schizophrenia and epilepsy.

As part of the routine protocol, for each subject presenting at the Center, extensive physical examination, spirometry, ECG are performed and biochemical tests are also collected, including Emocrome, Fibrinogen, C-reactive protein, Total cholesterol, HDL, LDL, Triglyceride, Serum creatinine, AST, ALT, Gamma-Glutamyltransferase, Glucose, Homocysteine, TSH, Glycated haemoglobin, Postprandial glycaemia, Insulin level, 2-hour post glucose insulin level, Urinary pH, Uric acid.

For the specific purpose of the present project each subject will be asked to:

- Sign an informed consent form explaining the study aims and procedures.
- 2 EDTA tubes blood samples (~15 ml)
- 1 PAXgene Blood RNA tube (~2,5ml)
- urine samples (~50 ml)
- hair sample (next to the root)

Each subject was administered a questionnaire to collect information on the major cardiovascular risk factors, in particular a lifestyle questionnaire and a diet questionnaire. The lifestyle questionnaire collects information on socio-demographic data, residential area (complete address, characteristics of the house, and traffic), education, past and present health status of the subjects and their first-degree relatives, medications in the last year, employment

history and for employed subjects address of the plant of their current work, smoking history, passive smoking at home and at workplace, physical activity levels and sedentary behavior, commuting time and transport mode.

The questionnaire on eating habits included questions on the number of servings from each food in a usual week or month. Several different types of food were investigated, including: legumes, vegetables, fruits, nuts, red and white meat, fish, eggs, dairy products, cereals, snacks, oil and butter, alcoholic beverage, tea and coffee. Number of servings from each food were translated into usual daily micronutrients intake weighting for serving size, age class and gender.

Both questionnaires were checked for completeness at the time of data collection in order to ensure high quality data.

EXPOSURE ASSESMENT

Exposure is defined using a multifaceted approach. In particular, PM_{10} is assigned to each subjects following two approaches: (1) use of daily PM_{10} concentration series from air quality monitors; (2) use of daily PM_{10} concentration estimates by the FARM model (the flexible air quality regional model), a three-dimensional Eulerian grid model for dispersion, transformation and deposition of particulates, capable to simulate PM_{10} concentration using a 4 km–dispersion grid.

1) Air Monitoring Stations

We collected recordings of daily PM₁₀ data by monitoring stations located at 154 different sites throughout Lombardy, with three of them located in the city of Milan (“Verziere”, “Pascal-Città Studi” and “Senato”). We used daily concentration measured by single monitors in the study area to characterize PM₁₀ exposure at the date of recruitment and until 365 days before, for each subject. Thus, we are able to estimate both short- and long-term exposure to the pollutant investigated. As air monitoring station recordings for the area of interest are available from 2001, older exposures might also be estimated.

We geocoded monitoring stations and study subject addresses to assign the latter daily PM₁₀ concentration from: (1) the monitor at the lower distance to home address, defined “subject’s residence”; (2) the nearest monitor to the Center for Obesity and Work (“Verziere”), defined “Policlinico”; (3) daily exposure for Milan created averaging the three available city monitors, defined as “average Milan”.

We assume that the day of the visit subjects are exposed to levels of PM₁₀ measured by the “Policlinico” station, as the time elapsed in the Hospital to perform all the examinations (approximately five hours) is supposed to be sufficient to experience outcomes related to very short-term effect. About 57% of SPHERE subjects live in the city and an additional 28% work in Milan (even if they live outside the city), overall a 67% of subjects spent many hours a day in the city or travelling from workplace to residence. Thus, longer exposure effects are evaluated by both residential and Milan monitors using appropriate lag time from recruitment date, as sensitivity analysis. However, very high correlation was observed among the three sources of exposition ($R_{\text{Policlinico}}$ vs

Average Milan=0.99; $R_{\text{Subjects' Residence vs Average Milan}}=0.94$; $R_{\text{Policlinico vs Subjects' Residence}}=0.99$).

2) FARM Eulerian Model

Estimated daily average concentrations of PM₁₀ for the years 2007-2013 based on the FARM Eulerian model were obtained from ARPA Lombardy. The FARM Eulerian model is a Chemical Transport Models (CTM) able to treat the main processes of chemical and physical nature of formation and removal of pollutants, in addition to the transport and dispersion by the action of wind and atmospheric mixing. By this model the Lombardy region was divided into a grid of 1678 cells (4x4 km), each associated with daily PM₁₀ concentration estimates. Hence each subject was attributed: (1) the estimated daily exposure of the cell containing their residential address; (2) the exposure of the cell containing the address of the Center for Obesity and Work; (3) the daily average exposure for Milan, calculated as the average of the 22 cells that falls into the city boundaries.

Eulerian model requires, as input data, emissions from area and point sources from emissions inventory (anthropogenic-mobile, industrial, commercial, domestic, rural sources); meteorology (wind, air temperature, pressure, relative humidity, cloud cover and height, precipitation, turbulent horizontal and vertical diffusivities, surface resistances and gas deposition velocities) and topography. Data elaborated by modeling systems integrates the ones of the monitoring network and allow to know air quality state on an extensive way on the territory. Thus, the advantage of Eulerian dispersion modeling, on

monitors, is that it allows to assess the population's risk of exposure to air pollution in regions where there are no direct observations. Data estimated from the models are available until 2012, since the data validation imply a lag time of nearly 6 months and will soon be available for further data analysis.

Considerations to keep in mind when comparing modelled and measured pollutants, are that models estimated mean concentration of a cell (16 Km), while monitors gave a punctual value which reflects the characteristics around the site and of the emissions sources.

PM₁₀ levels follows a seasonal trend. Critic periods are concentrated in autumn and winter seasons, which are characterized by atmospheric stability, calm wind and absence of precipitations. PM₁₀ air concentrations depends, besides emissions, on weather conditions during the days, in particular by rainfall, atmospheric stability and wind.

WORKFLOW PROCESS

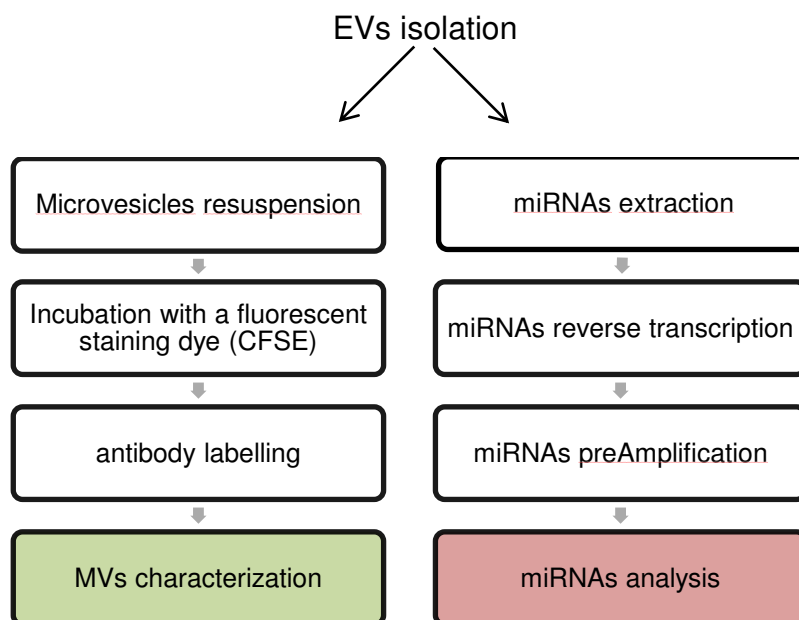


Figure 6. Workflow process in the two phases of the project.

EXTRACELLULAR VESICLES ISOLATION

Peripheral blood is collected in two EDTA tubes. We collect plasma fraction by centrifuging 2500 rpm for 15 minutes at room temperature. After centrifugation the intermediate stage (buffy coat), consisting mainly of lymphocytes and monocytes, was isolated and frozen. The EVs are then purified from plasma.

Plasma is centrifuged three times at 1000 x g, 2000 x g and 3000 x g for 15 minutes at 4°C, discarding the pellet to clean the cell debris.



Figure 7. BeckmanCoulter Optima-MAX-XP

The vesicles are then concentrated by ultracentrifugation (BeckmanCoulter Optima-MAX-XP) (Figure 7) at 110,000× g for 75min at 4°C.

EVs IMMUNOPHENOTYPING BY FLOW CYTOMETRY

The flow cytometry is a technique that allows the quantification and characterization of particles of biological origin due to their interaction with specific laser.

Over the years it has emerged as a technique for the evaluation of the cells, while today it is also widely used to determine the size, morphology and origin of extracellular vesicles [39].

The flow cytometry offers several advantages such as the possibility of multiparametric analysis, rapid analysis time (more than 1000 events / sec), reproducibility and statistical reliability of the measures.

For our study we used the MACSQuant Analyzers (Miltenyi

Biotech) (Figure 8),

with two lasers scatter (FSC, SSC) and eight channels for fluorescence.

The cells passage through the laser gives rise to a signal that is picked up by the sensor that collects light from the Forward scatter (FSC), giving



Figure 8. MACSQuant Analyzers- Miltenyi Biotech

information on the vesicular volume, and a further signal that is picked up by the side scatter (SSC) at 90 degrees, which provides information on the density / granularity of the vesicles.

In addition to these physical parameters has been possible to estimate biological parameters also thanks to

the use of molecules / antibodies conjugated to fluorochromes that emit fluorescence at different wavelengths.

FITC-carboxyfluorescein succinimidyl ester (CFSE) was used to

discriminate the integrity of the vesicles, as it is a vital dye, non-fluorescent molecule, capable of

entering the cytoplasm of MVs, where intracellular esterases remove the acetate group and convert the molecule in the ester fluorescent.

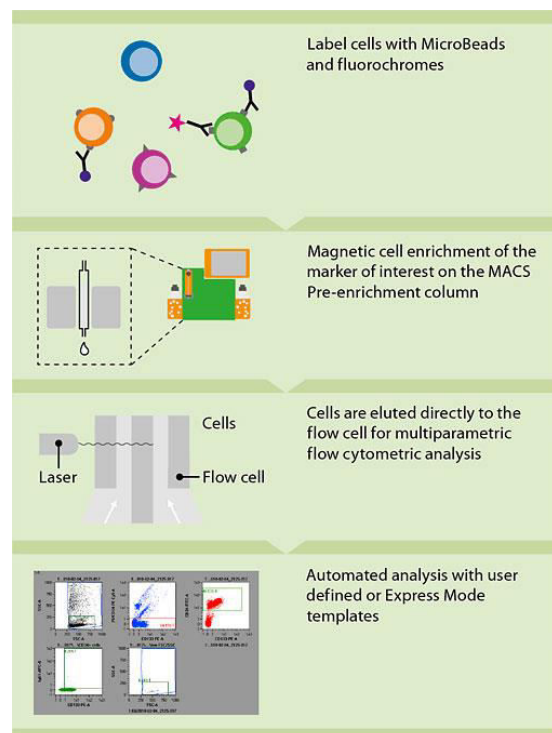


Figure 9. MACSQuant Analyzers operating principles

It is chosen, furthermore, to evaluate the presence of five subpopulations of microvesicles for each subject, through immunophenotyping with monoclonal antibodies capable of recognizing an epitope of a specific antigen (Figure 9).

We use antibody (Ab) CD61-APC to recognize MVs from platelets[96]; CD66-APC for MVs neutrophils; CD14-APC for MVs from monocytes[97]; CD105-APC for MVs by endothelium; EpCAM-APC for MVs epithelium[98].

We mark 350 μL of sample, resuspended with PBS three times filtered 0.10 μM , with 7 μL of Carboxy Fluorescein Succinimidyl Ester (CFSE) to reach a final solution concentration of 0.02 μM .

The samples are incubated at 37 ° for 20 minutes in the dark, to allow the activation of the fluorescent ester.

The samples labeled with CFSE are dispensed in 5 tubes each containing respectively 6 μL of one of the previously selected Abs: CD14, CD105, EpCAM, CD66 and CD61. Subsequently, the samples labeled with CFSE and antibody, are incubated for 20 minutes in the dark at 4 ° C to allow the activation of the Allophycocyanin(APC), the fluorophore conjugated to the antibody.

Before use, each antibody is centrifuged at 17000 g for 30 minutes at 4 ° C to eliminate the presence of aggregates.

We acquire 30 μL of sample double-labeled for multiparametric analysis by flow cytometry and the data obtained have allowed us to determine the concentration of intact double-positive microvesicles (CFSE +, APC +) and belonging to one of the five selected subpopulations.

In addition, before the analysis, it is estimated the output signal from PBS triple filtered unmarked, which was used for the suspension of microvesicles, to remove the background / noise of the buffer and make sure that it doesn't influence the analysis of samples and overestimate the concentration. The main limitation of the analysis is the small size and heterogeneity of the vesicles, between 0.1 and 1 micron, and the ability of the instrument in their detection.

For the vesicles, which have small dimensions when compared with the wavelength of the laser, is important a high sensitivity for both FSC and SSC . The scatter depends on the diameter, refractive index, absorption, and morphology of the vesicles, as well as by the wavelength of the laser. Generally, the vesicles are considered smooth spheres without absorption and it allows to determine their diameter knowing the wavelength of the laser and the refractive index. The limit is the the fact that the vesicles have a small range of refractive indices, between 1:36 and 1:40, for a wide range of sizes, from 190 to 1040 nm, and this makes it difficult to accurately assess their diameter.

This limit has been mostly superseded by the new flow cytometers, as MACSQuant analyzer, which have a scatter SSC able to discriminate with high accuracy vesicles between 160-220 nm.

We also improve the efficiency of the instrument with a double staining of MVs through markers fluorochrome-conjugated. To calibrate the instrument we use Fluoresbrite® Carboxylate Size Range Kit I, a mixture of polystyrene fluorescent microspheres with a size of 0.10µm, 0.20µm, 0.50µm, 0.75µm and 1.0µm.

To eliminate any kind of interference during the analyzes, the running buffer (containing a low concentration of salts), used to optimize the acquisition of the vesicles by the MACSQuant Analyzers, was filtered through a Millipore membrane 0.10 mM, to avoid the possible impurities present in the mixture. The cytometer shows us the results of the acquisition through cytograms.

Then we use FlowJo software for the analysis of these graphs, and to evaluate the characteristics of the vesicles. It allows us to organize and analyze samples, thus simplifying the statistical analysis and the creation of the gate for experiments with many samples, parameters and operations.

Figure 10 shows an example of cytograms in which we report the gating that identifies the MVs intact (CFSE+) and among these, the MVs positive to the antibody (eg CD61+).

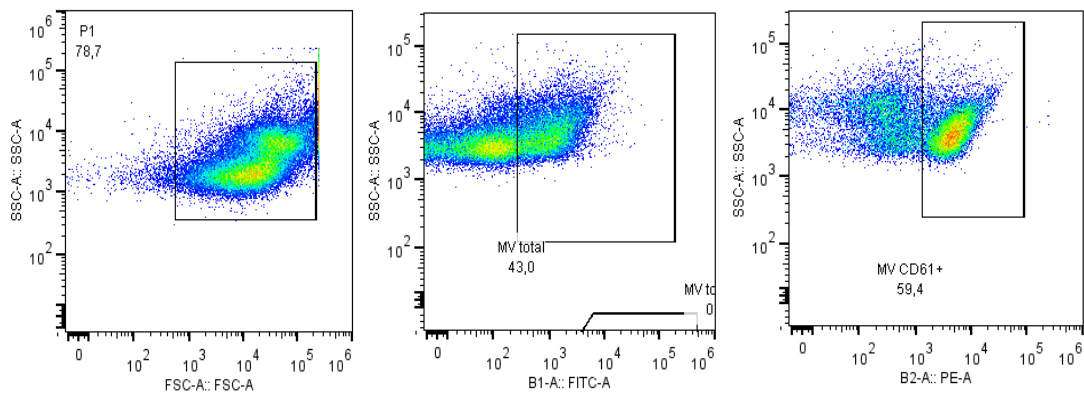


Figure 10. Cytograms of a MVs population, intact MVs and MVs positive to Ab CD61.

EVs COUNT AND SIZE

Nanoparticle Tracking Analysis (NTA) is a new method of analysis that can determine size and count of nano-particles suspended in a liquid. Thanks to an optical microscope with a red laser of 635 nm, it analyzes the Brownian motion of vesicles suspended in a fluid and displays them in real time through a CCD camera with high sensitivity (Figure 11).

The software is capable to display each particle and identify its center and position during the acquisition time. The image analysis allows to

calculate the average of the distance between the positions of each particle in motion along the axes x and y. Using the Stokes-Einstein equation we get diffusion coefficient (Δt) and consequently the diameter (d) of each nano-vesicle, knowing temperature (T) and viscosity (η) of the liquid:

$$Dt = \frac{K_B T}{3 \pi \eta d}$$

K_B is the Boltzmann constant.

Various studies have suggested that NTA is able to improve the capabilities of flow cytometry to analyze exosomes and microvesicles because it is possible to detect more vesicles in the range size between 35 and 251 nm using NTA in comparison to flow cytometry[99].

The accuracy of the calculation of the particle size by the software depends on several variables including the intrinsic characteristics of the particles, as the

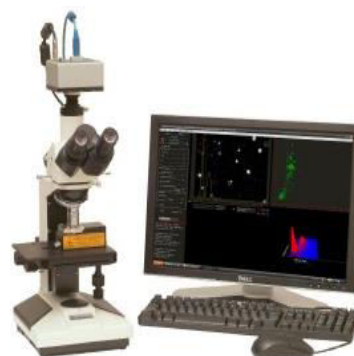


Figure 11. NanoSight LM10-HS

index of refraction.

For particles with a high refractive index, for example gold and silver in aqueous systems, we can get accurate dimensions up to 10 nm; for particles with a lower refractive index, such as those of biological origin, the smallest size well analyzable is between 25 and 35 nm.

However, the major limitation of the system is when the Brownian motion is so low that it does not allow to identify and track the center of the particle and its movements. This is typically observed for particles about 1-2 μ m in aqueous systems.

To optimize the analysis is often necessary to dilute the sample to allow the instrument to view the most of all the particles.

For our analysis were used 70 μ L of the sample to which were added 230 μ L of PBS three times filtered, to obtain a dilution of 4,28 : 1.

The sample is transferred, using a syringe, into a chamber of NanoSight LM10-HS (ultrahigh sensitive) and we make five different video captures (Figure 12).

Thanks to EMCCD camera (Electron Multiplication Charge Coupled Device), which has a higher sensitivity compared to the standard Nanosigh system, are recorded five movies of 30 seconds each to improve the statistical power of the analysis. The NanoSight analysis helps to overcome the limitations due to flow cytometry in the size estimation of vesicles.

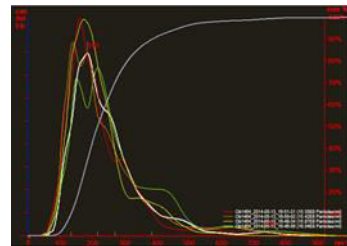
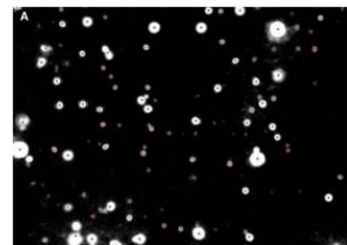


Figure 12. NTA operating principles

miRNAs EXTRACTION

miRNAs analysis and quantification requires a previous miRNAs extraction and purification phase. For this purpose we use miRNeasy Kit and RNeasy CleanUp Kit (Qiagen)

Procedure:

1. Add 700 μ l of QIAzol Lysis Reagent in each sample
2. Mix with pipette and transfer in a 2 ml tube
3. Vortex for 1 min
4. Place the tube at room temperature for 5 min
5. Add 140 μ l di chloroform and shake the tube vigorously for 15 s
6. Place the tube at room temp for 2-3 min
7. Centrifuge x 15 min at 12000 g at 8 °C.
8. Transfer the upper aqueous phase to a new collection tube
9. Add 350 μ l of 70% ethanol
10. Vortex
11. Transfer 700 μ l in a RNeasy spin column in a collection tube da 2 ml
12. Centrifuge at ≥ 10200 rpm for 15 s at 20°C
13. Trasfer the sample in a 2 ml tube(containing miRNA)
14. Throw spin column (except if you want to extract also totalRNA)
15. Add 450 μ l of 100% ethanol and vortex
16. Transfer 700 μ l of sample in a RNeasy MinElute spin column in a collection tube
17. Centrifuge for 15 s at ≥ 10200 rpm at 20°C

18. Transfer the spin column in a new collection tube
19. Transfer the remainder of the sample in the RNeasy MinElute spin column and repeat the centrifuge
20. Transfer in a new collection tube
21. Add 500 μ l of RPE Buffer in the RNeasy MinElute spin column and centrifuge for 15 sec at ≥ 10200 rpm
22. Transfer in a new collection tube
23. Add 500 μ l of 80 % ethanol and centrifuge x 2 min at ≥ 10200 rpm
24. Transfer the spin column in a new collection tube
25. Centrifuge with open lid for 5 min at ≥ 10200 rpm
26. Transfer spin column in a 1,5 ml tube and add 20 μ l of RNeasy free water
27. Wait for 5 min
28. Centrifuge x 1 min at ≥ 10200 rpm
29. Store at -80°C

miRNAs REVERSE TRANSCRIPTION

Reverse Transcription (RT) allows to produce cDNA starting from RNA and for this reason is exploited to study gene expression. For the analysis of miRNAs carried in plasma vesicles, we used 2 mix for each sample: one containing Megaplex RT primers Pool A v2.1 and the other one with Megaplex RT primers Pool B v3.0.

For miRNAs are used RT specific primers, called "stem-loop RT primers" , which contain a highly stable loop structure that extends the target cDNA (miRNA are too short for standard methods of RT-qPCR).

The Forward primer increases the length by adding additional nucleotides that optimize its melting temperature (T_m) and improve the test specificity. The Reverse primer destroys the loop structure. Furthermore, the steric hindrance due to the presence of the loop structure prevents primer binding to pri- or pre-miRNAs that may be present. Each RT reaction mix contains (Table 4):

RT Reaction Mix component	Volume	
Megaplex™ RT Primers (10X) (Pool A/Pool B)	0.75 µL	-Pool A: RT primers for 377 miRNAs and 4 control miRNAs (miRNAs best characterized and most expressed); -Pool B: RT primers for 377 miRNAs and 4 control miRNAs (miRNAs less characterized and / or expressed then Pool A).
dNTPS with dTTP (100mM)	0.15 µL	
MultiScribe Reverse Transcriptase (50U/µL)	1.50 µL	It 'a DNA-dependent RNA polymerase (reverse transcriptase), derived from Moloney Murine Leukemia Virus, which uses ssRNA as a template to synthesize one strand of complementary DNA (cDNA)
10X RT Buffer	0.75 µL	Buffer to maintain the pH stable; is required to establish the environment for the reaction.
MgCl ₂ (25Mm)	0.90 µL	It is used to add magnesium ions to the PCR reaction. Magnesium is a cofactor of the polymerase and its concentration affects its productivity.
RNase Inhibitor (20U/ µL)	0.1 µL	RNase inhibitor
Total	3.4 µL	

Table 4. Components of RT reaction mix

We aliquot 4,15µL of the RT reaction mix to each well of a 96-well plate (each sample is processed in two wells: one for pool A and one for pool B). Then we add 3.35 µL of RNA in each well containing the RT reaction mix and after we perform PCR reaction at the following conditions (Table 5):

Stage	Temp	Time
Hold	95 °C	10 min
Hold	55 °C	2 min
Hold	72 °C	2 min
Cycle (16 Cycles)	95 °C	15 sec
	60 °C	4 min
Hold*	99.9 °C	10 min
Hold	4 °C	∞

Table 5. PCR conditions

REAL TIME-PCR

The product of the preamplification reaction was diluted 1/20. The Real Time PCR reaction was prepared with "TaqMan Open Array Real Time PCR MasterMix".

We transferred the reaction product (7µl), using a Robot Let Microlab STAR (Hamilton Robotics) from the plate 96 to 384. Finally through the AccuFill™ Robot System (Life Technologies) we set up the Open Array Plate consists of 48 subarrays with 64 holes, for a total of 3072 holes of diameter 300 µM and 300 µM of depth (Figure 13).

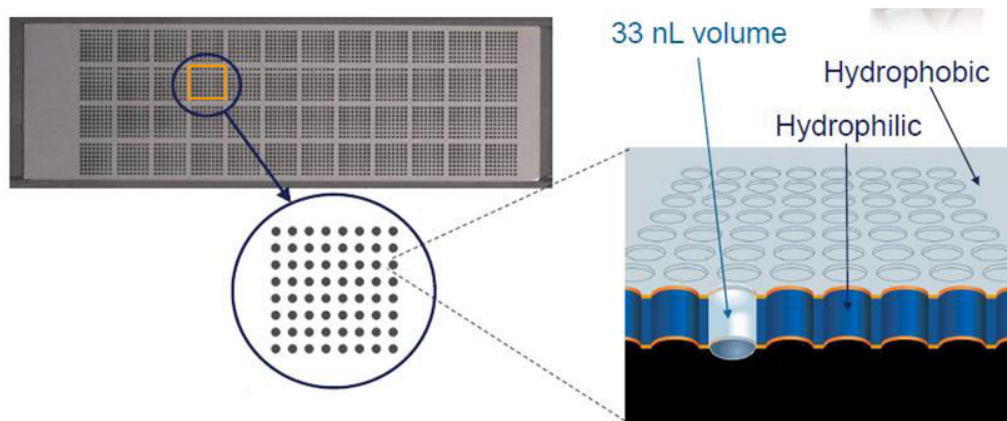


Figure 13. OpenArray plate

Each hole has an outer hydrophobic coating, while inside is hydrophilic (the reagents are kept inside by surface tension) . In this way each reaction of real time PCR has a final volume of 33 nanoliters.

After loading the sample, we covered the plate with adhesive Lid and filled with immersion fluid. The plate is loaded into *QuantStudio™ 12K Flex OpenArray* (Life Technologies) (Figure 14) that allows the simultaneous analysis of up to 4 OpenArray plates, for a total of 12 samples (3 per plate).



Figure 14. QuantStudio™ 12K Flex OpenArray

The Real-Time PCR, also called quantitative PCR or real-time quantitative PCR (RTQ-PCR), is a method of amplification (polymerase chain reaction or PCR) and simultaneous quantification of DNA samples and cDNA.

The fluorescence, generated during PCR, is the result of several possible chemical reactions.

The main chemistries are based on the binding of fluorescent dyes that intercalate into the double helix of DNA, such as SYBR Green, or on the hybridization of specific probes, such as TaqMan probes. In this experiment, we used the TaqMan probes. The use of probes revealing fluorescence is one of the most accurate and reliable methods, as the TaqMan probes are designed to pair up to specific target sequences.

A typical cycle of real-time PCR

1. Denaturation of template DNA (94-99°C).
2. Annealing of the oligonucleotides to the sequence (30-65°C).
3. Extension by DNA polymerase starting from the heat-resistant primers (65-72°C).

The Real-Time PCR is quantitative, as the data are collected during the exponential growth phase, when the quantity of the reaction product is directly proportional to the initial amount of nucleic acid.

The quantification of the miRNA is based on the fluorescence detected at each reaction cycle: at each cycle, the cDNA molecules are doubled, up to reach a plateau when the reagents are exhausted and the enzyme activity decreases drastically.

The instrument software provides data analysis of the results:

1) Relative ThresholdCycle (C_{rt}) (Figure 15): represents the number of PCR cycles at which the efficiency of the reaction of Real-Time PCR miRNA target is maximal. This data is used to quantify the initial target miRNA. The higher the C_{rt}, the lower the expression of miRNAs.

2) Ampscore: one of the most important parameters that we used to evaluate the goodness of the reaction. A good amplifier has an Ampscore greater than 1.24. This means that the curve representing its amplification, as a result of the Real-Time PCR, has the characteristic of an exponential growth curve. With this information, determine the amp score can also help to discriminate false positives and false negatives.

Unlike the Ct method, which considers all the curves for a specific target to determine the threshold, the Crt method sets a threshold for each curve individually that is based on the shape of the amplification curve, regardless of the height or variability of the curve in its early baseline fluorescence. The method first estimates a curve that models the reaction efficiency from the amplification curve. It then uses this curve to determine the relative threshold cycle (Crt) from the amplification curve. The Crt algorithm computes a Cq that is roughly in the middle of the exponential growth region.

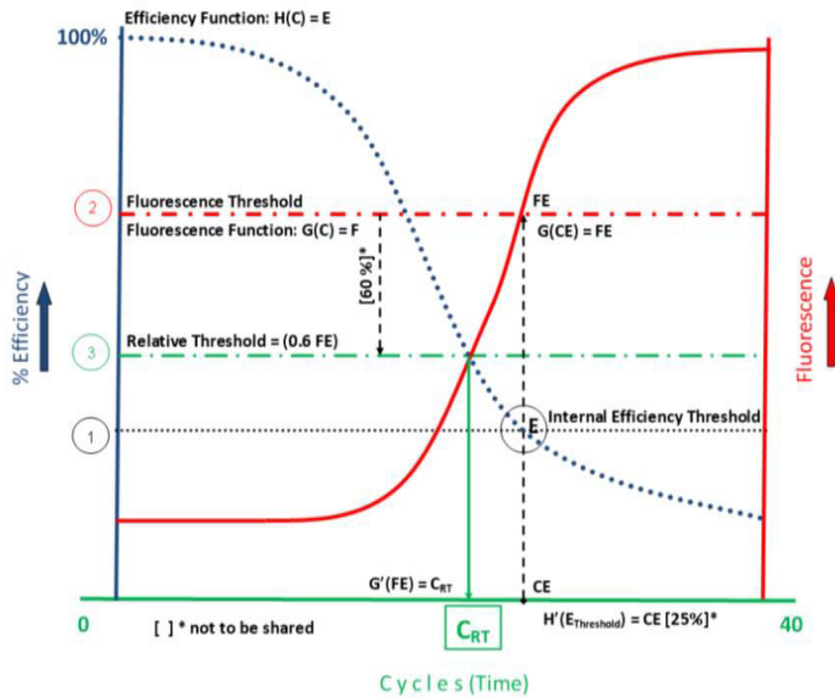


Figure 15: Relative Threshold Cycle (Crt)

The analysis of the results was carried out with the program Expression Suite. We have selected the reactions up to the 28th cycle of RTq-PCR, as hypothetical amplifications occurred in subsequent cycles are irrelevant for the study.

RESULTS

STUDY SUBJECT CHARACTERISTICS

The population examined in this study includes 1250 subjects recruited at 31 December 2013, 87% of whom living in the province of Milan. In particular we recruited 883 subjects for miRNAs study (recruited from 2010 till 2012) and 266 (recruited from January till November 2013) subjects for MVs characterization.

We structured the study in two phases to better investigate both the cellular origin of microvesicles both their content in terms of miRNAs.

The characteristics of the study population in the two different phases of this study (miRNAs analysis and MV characterization) are similar and reflect those of the entire population (Table 6 and Table 7).

The study population is recruited at the Center for Obesity and Work (*IRCCS Fondazione Ca'Granda Ospedale Maggiore Policlinico*). The participation rate was 90%. Mean BMI of our study population is 33.5 Kg/cm² (± 5.5): nearly 27.8% are overweight, 38.6% are obese, and 33.6% severe obese.

The percentage of obese individuals in Lombardy is about 10.3% of the total adult population. The condition of overweight/obesity in Italy increases with age, is more common in men and among people with lower education and most economically disadvantaged. (*Fonte Rapporto sui fattori di rischio in "Noi Italia" di ISTAT*)

The study population is composed by 74% of female, mean aged 52 years.

Characteristics	Categories	n=1250
Sex	Male	330 (26.4%)
	Female	920 (73.6%)
Age	Years (mean±SD)	51.9±13.6
Education	Primary school or less	105 (8.4%)
	Secondary school	325 (26.0%)
	High school	493 (39.4%)
	University	188 (15.0%)
	Others	87 (7.0%)
	Missing	52 (4.2%)
Occupation	Employee	714 (57.1%)
	Unemployed	102 (8.2%)
	Pensioner	304 (24.3%)
	Housewife	93 (7.4%)
	Missing	37 (3.0%)
Ethnicity	White	1198(95.8%)
	Black	11 (0.9%)
	Asian	3 (0.3%)
	South America	38 (3.0%)
Year of enrollment	2010	129 (10.3%)
	2011	419 (33.5%)
	2012	385 (30.8%)
	2013	317 (25.4%)
Season of enrollment	Winter	320 (25.6%)
	Spring	313 (25.0%)
	Summer	190 (15.2%)
	Autumn	427 (34.2%)
Smoking	Never	599 (47.9%)
	Former	431 (34.5%)
	Current	190 (15.2%)
	Missing	30 (2.4%)
Cigarettes smoked*	<= 5	53 (27.9%)
	5-10	53 (27.9%)
	10-15	33 (17.4%)
	15-20	37 (19.6%)
	20-40	13 (6.8%)
	Missing	1 (0.5%)
Time since quitting (n=419)	Median [Q1, Q3]	13.1 [5.8-23.4]

Pack/years (n=1153) Among current and former Including nonsmokers	Median [Q1, Q3]	14.5 [6.1-28.0] 0 [0-13.5]
Alcohol consumption	Yes	636 (50.9%)
	No	518 (41.4%)
	Missing	96 (7.7%)
Residence area	City	534 (42.7%)
	Peripheral area	331 (26.5%)
	Rural area	30 (2.4%)
	Village/small city	206 (16.5%)
	Missing	149 (11.9%)
Living area	Province of Milan (Excluding City of <i>City of Milan</i>)	379 (30.3%) 713 (57.0%)
	Outside Milan	158 (12.7%)
Work area	Province of Milan (Excluding City of <i>City of Milan</i>)	94 (13.1%) 339 (47.5%)
	Outside Milan	34 (4.8%)
	Missing	247 (34.6%)
Floor of residence	Ground floor	223 (17.8%)
	First floor	244 (19.5%)
	Second floor	156 (12.5%)
	Beyond second floor	471 (37.7%)
	Missing	156 (12.5%)
Residence traffic exposure	Mild	108 (8.7%)
	Moderate	595 (47.6%)
	Heavy	369 (29.5%)
	Missing	178 (14.2%)

Table 6. Characteristics of study participants and data collected from the self-reported questionnaire

Characteristics	N	
BMI, Kg/cm ²	1247	33.5±5.5
BMI categorical		
<30 Kg/cm ²		347 (27.8%)
30-35 Kg/cm ²		483 (38.6%)
≥35 Kg/cm ²		420 (33.6%)
Waist circumference, cm	1237	101.3±13.1
Blood pressure, mmHg	1247	
Systolic		125.4±15.8
Diastolic		78.5±9.5
Above 140/90 mmHg		60 (4.8%)
Below 140/90 mmHg		1190 (95.2%)
Heart rate, bpm	1243	67.6±10.4
Uric acid	1163	5.2±1.4
Fibrinogen, mg/dl	1129	335±59
C-reactive protein	1160	0.3 [0.1-0.5]
Total cholesterol, mg/dl	1165	215.1±41
HDL		59.2±15.5
LDL		134.7±36.3
Triglyceride	1164	107 [77-145.5]
Serum creatinine, mg/dL	1165	0.8±0.3
AST, U/l	1159	19 [16-23]
ALT, U/l	1160	21 [16-30.5]
Gamma-Glutamyltransferase, IU/L	1162	19 [13-30]
Glucose	1155	92 [86-101]
Homocysteine	1151	10.4 [8.6-12.7]
TSH	1163	1.7 [1.2-2.5]
Glycated hemoglobin, mmol/mol	1159	39 [36.6-43]
Postprandial glycaemia, mg/dl	1162	99 [90-112]
Insulin level	1158	12.3 [8.8-18]
2-hour post glucose insulin level	1155	46.4 [27.6-73]
Urinary pH	1144	5.6±0.7
Emocrome	1156	
White blood cells		6.8±1.7
Red blood cells		4.8±0.4
Hemoglobin		13.8±1.4
Hematocrit		40.7±3.4
Mean Corpuscular Volume		85.1±6.4
Platelets		249.7±59

Table 7. Characteristics of the study subjects and mean levels of the clinical measure

COMPARISON BETWEEN FARM MODEL AND MONITORING STATION PM₁₀ LEVELS.

Air quality modeling and ambient measurements are two different ways to estimate actual ambient concentrations of pollutants in the atmosphere. Both modeling and measurements have some degree of uncertainty associated with their estimates.

Figure 16 shows the distributions of daily mean PM₁₀ concentrations of all monitors and of all grid cells with a monitor falling into their boundary. Darker area highlights winter months, characterized by major differences between the two methods of exposure assessment.

The winter months (October to February) are those where there is a more obvious difference between the two methods of exposure assessment; for the rest of the year the distributions are similar.

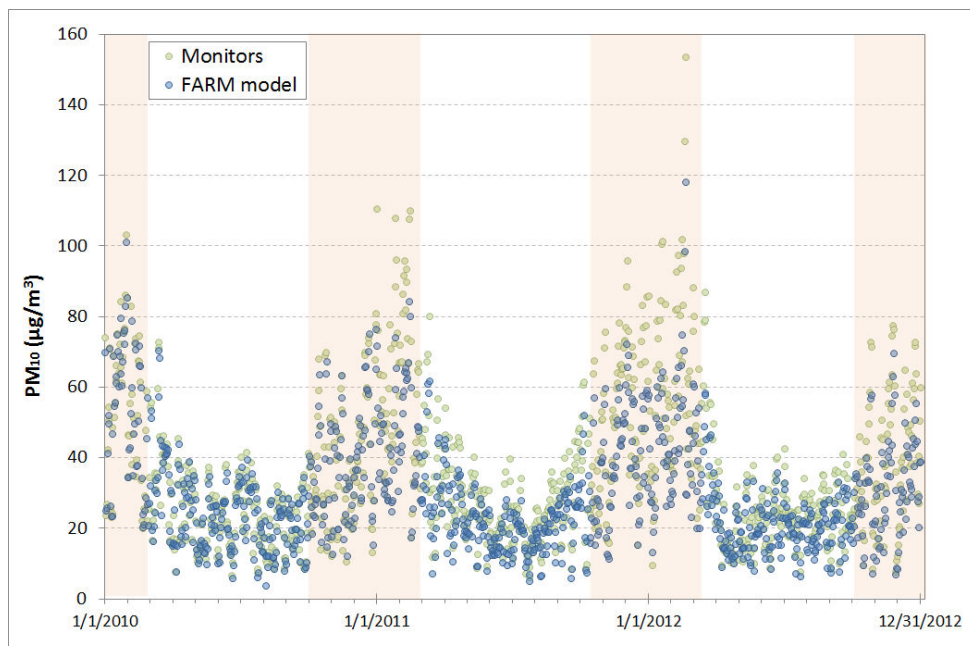


Figure 16. Daily mean PM₁₀ concentrations of all monitors and of all grid cells with a monitor falling into their boundary. Darker area highlights winter months, characterized by major differences between the two methods of exposure assessment

The differences between the two methods are consistent with what reported by ARPA Lombardy in the Annual Assessment Of Air Quality Modeling for years 2009-2011.

We can summarize as follows the pros e cons of using PM₁₀ exposure from FARM model air and from monitoring stations:

FARM model:

- ✓ provides an estimate of PM₁₀ for a grid of 1678 cells 4x4Km;
- ✓ no missing values in PM₁₀ series;
- ✓ is not easy to obtain (formal request to ARPA Lombardy);
- ✓ validation requires long times (7-8 mesi);
- ✓ high complexity of the model and the variables that feed it;

Monitoring Stations:

- ✓ easy availability from the site ARPA air quality;
- ✓ validation times from 3 to 6 months, but not validated series are also available;
- ✓ provides a punctual PM₁₀ measure by 81 air monitoring stations;
- ✓ lengthy procedure of estimation of missing data that is not always possible when the number of missing is high.

In conclusion, individual air pollution exposure assessment is determined using two sources of information:

actual monitor measurements for each and every day starting from January 1st, 1990 and a regional well validated modelling systems applied starting from 2007.

We decide to use FARM model data exposure for the analysis of the association between PM₁₀ exposure and miRNAs expression.

Instead for the analysis of the association between PM₁₀ and MVs subpopulation we used mean PM₁₀ concentrations measured by the three Monitoring Stations in the city of Milan, this was necessary due to the lack of data from the FARM Eulerian model.

ASSOCIATION BETWEEN PM₁₀ , EVs AND MVs SUBPOPULATION

To assess the association between PM₁₀ exposure and microvesicles concentration we use a multivariate statistical model adjusted for sex, BMI, interaction between PM₁₀ and BMI and apparent temperature.

The apparent temperature was calculated using the Kalkstein and Valimont formula :

$$Ta = -2653 + (0994 * T) + (0.0153 * Dew ^ 2)$$

where T is the temperature in Celsius degrees and Dew is the dew point.

The study subpopulation consists of 266 subjects recruited from January 2013 till November 2013.

In this phase of the study we are attributing to each subject the PM₁₀ exposure estimated in the center of Milan area using the mean of PM₁₀ values measured by the three ARPA monitoring station (via Pascal, via Verziere, via Senato) , the blood drawing day.

Association between PM ₁₀ and EVs					
Microvesicles	Δ %	IC 95%	P-value	β	SE
MVs _{CD61+}	6,6	(1.7; 11.6)	0,008	0.0637	±0.024
MVs _{CD66+}	3,4	(0.3; 6.7)	0,033	0.0338	±0.016
MVs _{EPCAM+}	3	(-0.5; 6.5)	0,097	0.0292	±0.017
MVs _{CD105+}	3,9	(0.3; 7.6)	0,034	0.0389	±0.018
MVs _{CD14+}	7	(2.6; 11.5)	0,002	0.0675	±0.021
MVs total	2,8	(0.7; 5.0)	0,010	0.0279	±0.011
Exosomes total	1,1	(-3.2; 5.6)	0,626	0.0109	±0.022

Table 8. Association between PM₁₀ exposure and microvesicles concentration adjusted for sex, BMI, interaction between PM₁₀ and BMI and apparent temperature.

As shown in Table 8, there is a 6.6% increase in the concentration of MVs CD61 + (from platelets); 3.4% for MVs CD66 + (neutrophils); 3.9% MVs for CD105 + (endothelium); 7% for MVs CD14 + (monocytes); while there is no significant association for MVs EpCAM + (from pulmonary epithelium); where Δ represents $(\exp(\beta) - 1)\%$ and indicates the percentage increase of MVs concentration with an increase of $1 \mu\text{g} / \text{m}^3$ of PM₁₀.

Here the graphical results presented in terms of \ln (MV subpopulation) in relation to the mean value of PM₁₀ in the city of Milan (Figure 17).

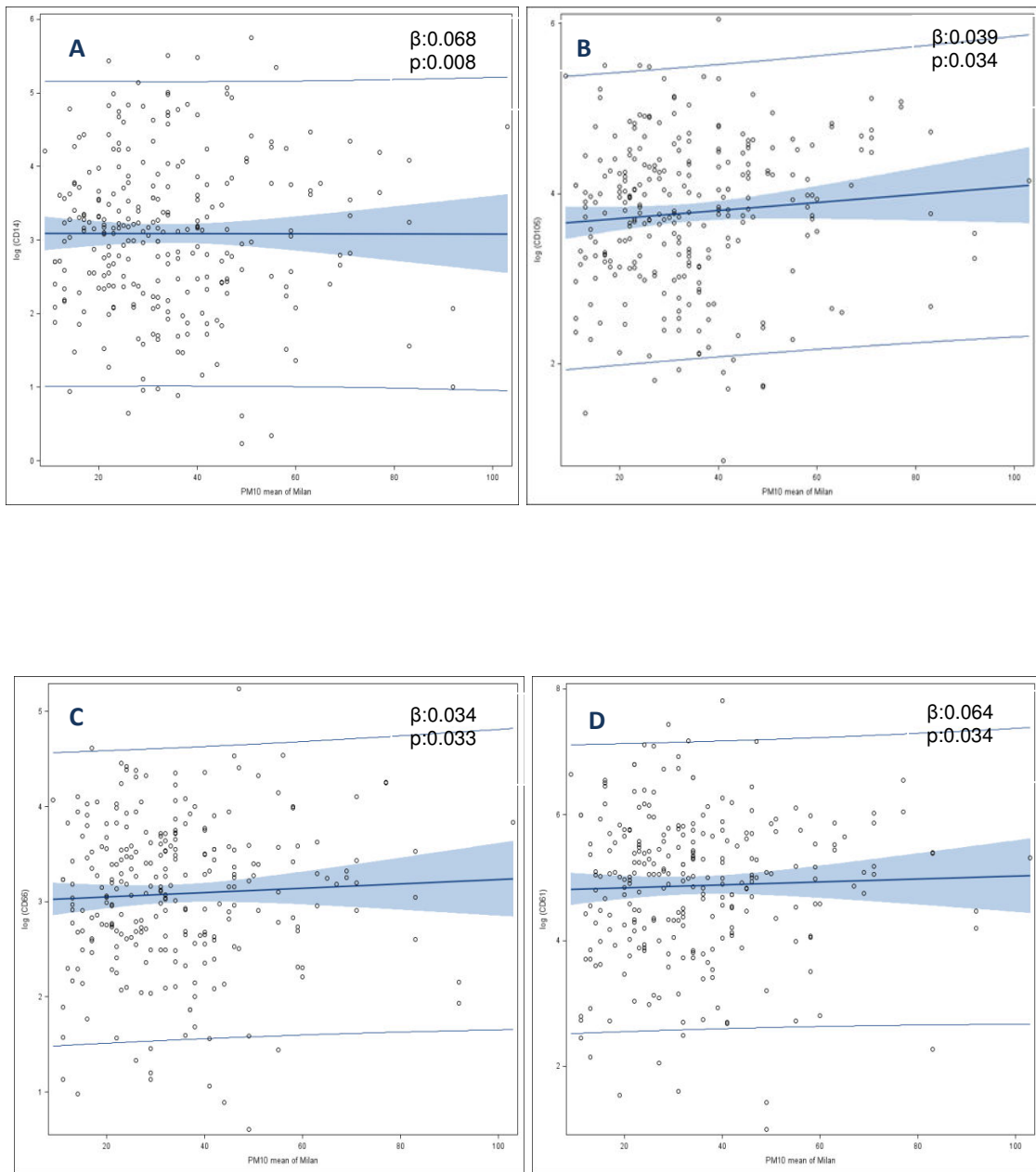


Figure 17. Association between the Milan mean daily exposure (averaging the three available city monitors) of PM₁₀ and MVs CD14+ (Panel A), MVs CD105+ (Panel B), MVs CD66+ (Panel C), MVs CD61+ (Panel D). Adjusted for sex, body mass index, interaction of BMI and PM₁₀ and apparent temperature.

INTERACTION BETWEEN PM₁₀ AND OBESITY

The average value of PM₁₀ (derived from the average of PM₁₀ values measured by the three ARPA stations in the city of Milan, the blood drawing day) is 34.29 mg / m³ (SD ± 16.7); the minimum value is 9 g / m³; median 31.5 g / m³ and maximum value 103 µg / m³.

Scientific evidence attests the link between obesity and environmental pollution, stating that the obese individuals are more susceptible to PM₁₀ exposure, as discussed previously, so we test the interaction of the BMI values between PM₁₀ exposure and microvesicles concentration.

We observe an interaction between the PM₁₀ and the BMI value of the different subjects (Figure 18). For each value of PM₁₀, as the value increases in body mass index, we observe an increase in microvesicles release for all the subpopulation analyzed, CD61+ (platelets), CD66+ (neutrophils), CD105+ (endothelium), CD14+ (monocytes) and EpCAM+ (lung epithelium); so, at the same PM₁₀ concentration, the overweight subjects with BMI 24-30 have less microvesicles than obese with a BMI ≥ 30.

This means that the association between PM₁₀ and plasma microvesicles seems to be conditioned by body mass index.

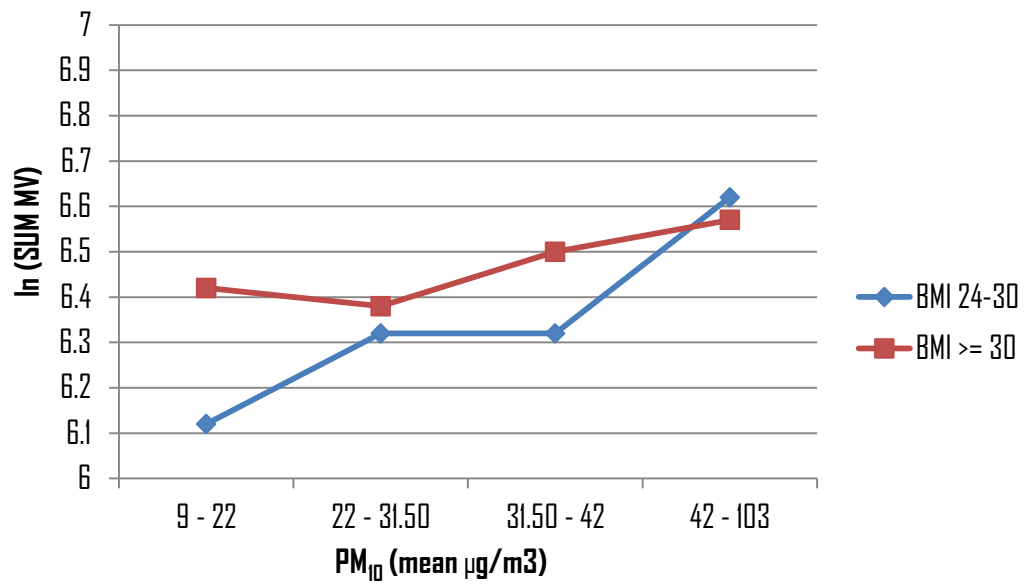


Figure 18. Interaction between PM₁₀ and BMI

ASSOCIATION BETWEEN miRNAs EXPRESSION AND PM₁₀ EXPOSURE

In order to verify the association between miRNAs expression and PM₁₀ we first fitted multiple linear regression models. As exposure was considered the daily PM₁₀ exposure estimate ($\mu\text{g}/\text{m}^3$) from Eulerian model for the 4x4 km cell containing the address of the Center for Obesity and Weight Control. The exposure lag period chosen for the analysis is of zero days (daily exposure of blood collection day). As outcome was considered the Relative quantification RQ of each miRNAs. log₂ transformation was applied in order to satisfy the normality assumption of linear regression model. False discovery rate control (FDR) was applied to control the expected proportion of incorrectly rejected null hypothesis in multiple comparisons (threshold of 0.10). The following adjusting variables were selected: sex, age, body mass index, cigarette smoking (never, former, or current). We also adjusted for seasonality (using sine and cosine) and apparent temperature.

In Table 9 is shown the association between FARM model estimate of PM₁₀ daily exposure and miRNAs expression. Have been reported the first 52 miRNAs, all statistically significant, because they are those that will be examined in a second phase of validation study in Real Time PCR on a further 1000 subjects. In Figure 19 are shown the graphical results of the association between eulerian estimate of PM₁₀ daily exposure and miR106a, miR152, miR218 expression (adjusted for age, sex, body mass index, cigarette smoking, date, Seasonality and apparent temperature).

	Estimate β	StdErr	LowerCL	UpperCL	Raw pvalues	FDR pvalues
miR-106a	-0,01224	0,00241	-0,01697	-0,00751	0,00000	0,00000
miR-152	-0,01315	0,00320	-0,01943	-0,00687	0,00000	0,00000
miR-218	-0,01462	0,00351	-0,02150	-0,00774	0,00000	0,00000
miR-27b	-0,01655	0,00379	-0,02399	-0,00912	0,00000	0,00000
miR-30d	-0,01560	0,00354	-0,02254	-0,00866	0,00000	0,00000
miR-652	-0,02350	0,00502	-0,03336	-0,01364	0,00000	0,00000
miR-92a	-0,01135	0,00276	-0,01677	-0,00594	0,00000	0,00000
miR-181a-2	-0,01487	0,00387	-0,02246	-0,00728	0,00010	0,00351
miR-25	-0,01225	0,00308	-0,01829	-0,00621	0,00010	0,00351
miR-375	-0,01757	0,00437	-0,02614	-0,00900	0,00010	0,00351
miR-720	-0,01085	0,00275	-0,01624	-0,00546	0,00010	0,00351
miR-9	-0,01555	0,00387	-0,02314	-0,00796	0,00010	0,00351
let-7c	-0,01423	0,00379	-0,02167	-0,00678	0,00020	0,00479
miR-1274B	-0,01171	0,00309	-0,01778	-0,00564	0,00020	0,00479
miR-24	-0,00921	0,00248	-0,01408	-0,00435	0,00020	0,00479
miR-28	-0,01487	0,00397	-0,02267	-0,00707	0,00020	0,00479
miR-99b	-0,01209	0,00321	-0,01839	-0,00579	0,00020	0,00479
let-7g	-0,01264	0,00348	-0,01946	-0,00581	0,00030	0,00479
miR-136	-0,01500	0,00411	-0,02306	-0,00693	0,00030	0,00479
miR-18a	-0,01275	0,00353	-0,01968	-0,00581	0,00030	0,00479
miR-20a	-0,01357	0,00375	-0,02093	-0,00620	0,00030	0,00479
miR-27a	-0,01276	0,00348	-0,01959	-0,00593	0,00030	0,00479
miR-331	-0,01069	0,00292	-0,01642	-0,00497	0,00030	0,00479
miR-744	-0,01352	0,00376	-0,02090	-0,00615	0,00030	0,00479
miR-590-3P	-0,01442	0,00414	-0,02255	-0,00628	0,00050	0,00712
miR-20a	-0,00969	0,00286	-0,01531	-0,00407	0,00070	0,00878
miR-22	-0,01349	0,00398	-0,02130	-0,00568	0,00070	0,00878
miR-423-5p	-0,01235	0,00364	-0,01951	-0,00520	0,00070	0,00878
let-7d	-0,01584	0,00468	-0,02503	-0,00665	0,00080	0,00980
miR-184	-0,01485	0,00444	-0,02356	-0,00614	0,00090	0,01054
miR-766	-0,01148	0,00344	-0,01824	-0,00472	0,00090	0,01054
miR-301b	-0,01262	0,00381	-0,02010	-0,00515	0,00100	0,01146
miR-340	-0,01264	0,00387	-0,02024	-0,00504	0,00110	0,01233
miR-126	-0,01520	0,00469	-0,02440	-0,00599	0,00120	0,01291
miR-185	-0,01022	0,00319	-0,01649	-0,00395	0,00140	0,01366
miR-340	-0,01345	0,00420	-0,02168	-0,00521	0,00140	0,01366
miR-625	-0,01705	0,00531	-0,02749	-0,00662	0,00140	0,01366
miR-598	-0,01223	0,00383	-0,01974	-0,00471	0,00150	0,01405

miR-125b	-0,01045	0,00329	-0,01692	-0,00399	0,00160	0,01405
miR-127	-0,01450	0,00457	-0,02347	-0,00553	0,00160	0,01405
miR-26b	-0,00945	0,00298	-0,01531	-0,00360	0,00160	0,01405
miR-505	-0,01185	0,00381	-0,01932	-0,00438	0,00190	0,01615
miR-143	-0,01187	0,00382	-0,01937	-0,00437	0,00200	0,01652
miR-148b	-0,01331	0,00432	-0,02179	-0,00483	0,00210	0,01652
miR-186	-0,01144	0,00370	-0,01870	-0,00417	0,00210	0,01652
miR-642	-0,01275	0,00413	-0,02085	-0,00464	0,00210	0,01652
miR-638	-0,01745	0,00568	-0,02859	-0,00631	0,00220	0,01680
miR-148a	-0,02181	0,00716	-0,03587	-0,00775	0,00240	0,01686
miR-17	-0,00971	0,00318	-0,01596	-0,00346	0,00240	0,01686
miR-223	-0,00661	0,00218	-0,01088	-0,00233	0,00250	0,01734
miR-19b	-0,00750	0,00248	-0,01237	-0,00262	0,00260	0,01757
miR-224	-0,01370	0,00459	-0,02272	-0,00468	0,00290	0,01935

Table 9. Association between FARM model estimate of PM₁₀ daily exposure and miRNAs expression adjusted for age, sex, body mass index, cigarette smoking, date, seasonality (using sine and cosine) and apparent temperature. Only the first 52 miRNAs with FDR pValue < 0.1 are shown.

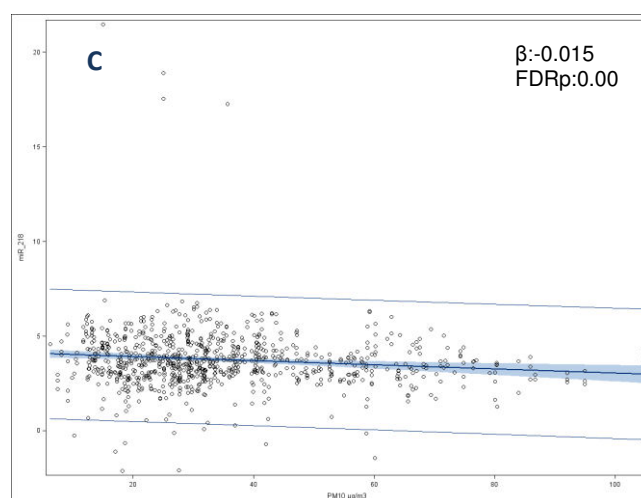
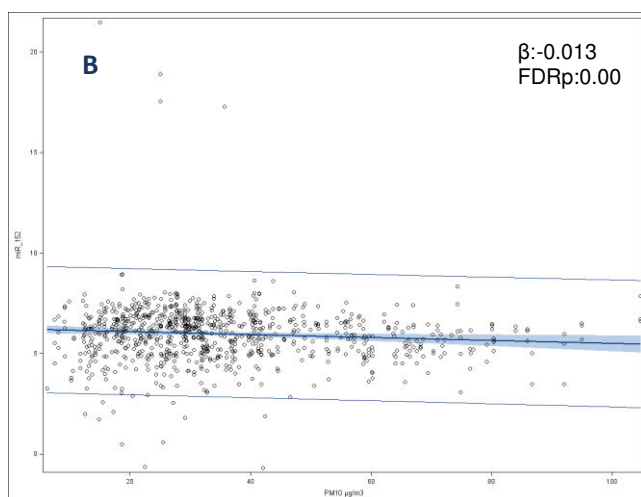
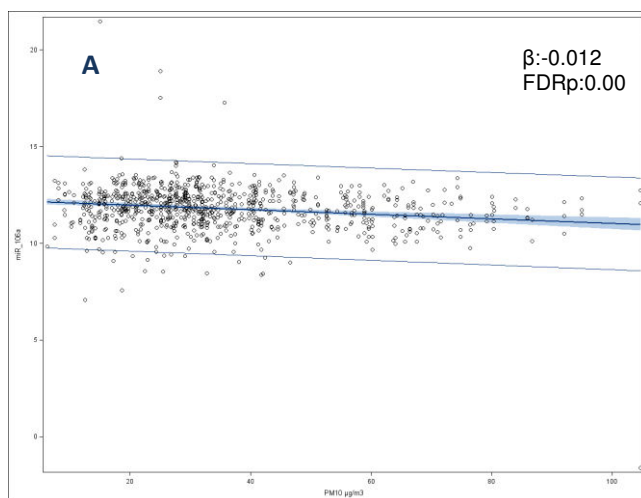
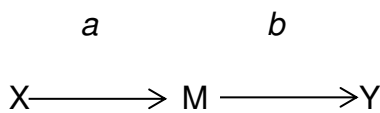


Figure 19. Association between eulerian estimate of PM₁₀ daily exposure and miR-106a (Panel A), miR-152 (Panel B), miR-218 (Panel C) expression adjusted for age, sex, body mass index, cigarette smoking, date, Seasonality (using sine and cosine) and apparent temperature.

MEDIATION ANALYSIS TO INVESTIGATE THE ROLE OF miRNAs EXPRESSION AS MEDIATOR OF THE EFFECT OF PM₁₀ ON CARDIAC OUTCOMES:SYSTOLIC AND DIASTOLIC BLOOD PRESSURE.

Mediation is a hypothesized causal chain in which one variable affects a second variable that, in turn, affects a third variable. The intervening variable, M, is the mediator. It “mediates” the relationship between a predictor, X, and an outcome. Graphically, mediation can be depicted in the following way:



Paths *a* and *b* are called direct effects. The mediational effect, in which X leads to Y through M, is called the indirect effect. The indirect effect represents the portion of the relationship between X and Y that is mediated by M.

The hypothesis underlying this analysis is that miRNAs expression can acts as mediator effect of the total effect of the exposure variable PM₁₀ on cardiac functions measured by respectively Systolic (Table 10) and Diastolic Blood Pressure (Table 11).

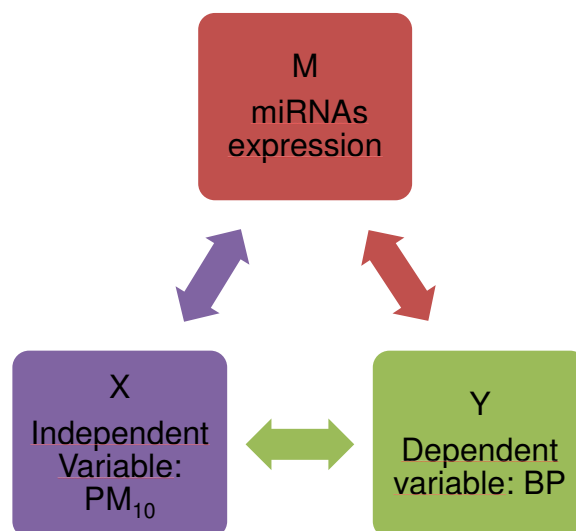


Figure 20. Simple mediation model

Figure 20 represents a simple mediation model where, a is the coefficient for X (PM_{10}) in a model predicting the mediator M (miRNAs expression) from X , and b and c are the coefficients in a model predicting the Y (blood pressure) from both the mediator M and X , respectively.

Is a four step approach in which several regression analyses are conducted and significance of the coefficients is examined at each step (Figure 21).

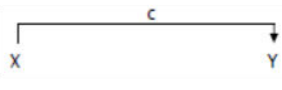
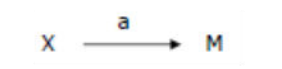
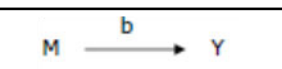
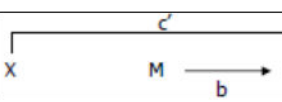
	Analysis	Visual Depiction
Step 1	Conduct a simple regression analysis with X predicting Y to test for path c alone, $Y = B_0 + B_1X + e$	
Step 2	Conduct a simple regression analysis with X predicting M to test for path a , $M = B_0 + B_1X + e$.	
Step 3	Conduct a simple regression analysis with M predicting Y to test the significance of path b alone	
Step 4	Conduct a multiple regression analysis with X and M predicting Y , $Y = B_0 + B_1X + B_2M + e$	

Figure 21. Causal steps approach

If one or more of these relationships are non-significant, researchers usually conclude that mediation is not possible or likely.

Systolic Blood Pressure			
miRNAs	Indirect Effect	Sobel test p-value	Proportion Mediated (%)
miR 106a	0.010	0.04	36.83
miR 152	0.001	0.756	2.70
miR 181a	0.007	0.118	25.31
miR 218	-0.005	0.172	17.94
miR 27b	0.002	0.339	7.22
miR 30d	0.002	0.483	8.08
miR 652	0.003	0.389	11.20
miR 92a	0.004	0.189	13.50
miR 25	0.002	0.483	6.23
miR 375	0.005	0.231	17.49

Table 10. Mediation analysis of the effect of exposure to PM₁₀ on Systolic Blood Pressure (SBP) through miRNAs expression.

There are the conditions to state that miR106a expression explains SBP when controlling for PM₁₀ and that the data are consistent with the hypothesis that miR106a expression fully mediates the relationship between PM₁₀ and SBP. Finally, the Sobel tests is significant ($p=0.015$), indicating that the mediation pathway (operated by miR106a) is statistically significant. Moreover we can estimate that percent of the total effect that is mediated is about 36.8% and an indirect effect of 0.010.

No miRNAs seems to act as mediator of the effect of PM₁₀ on Diastolic Blood Pressure.

Diastolic Blood Pressure			
miRNAs	Indirect Effect	Sobel test p-value	Proportion Mediated (%)
miR 106a	0.002	0.536	8.89
miR 152	0.001	0.676	2.83
miR 181a	0.003	0.285	12.86
miR 218	-0.002	0.330	9.44
miR 27b	0.002	0.230	7.98
miR 30d	-0.001	0.597	4.65
miR 652	0.003	0.150	15.32
miR 92a	-0.0002	0.855	1.22
miR 25	0.0001	0.99	0.04
miR 375	0.002	0.476	7.78

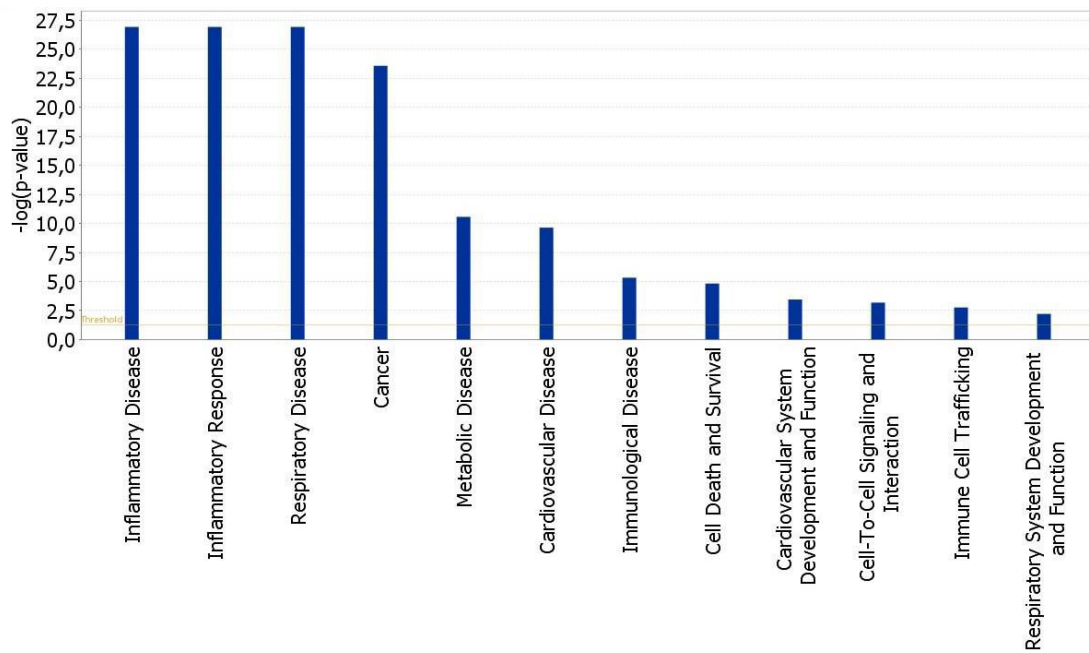
Table 11. Mediation analysis of the effect of exposure to PM₁₀ on Diastolic Blood Pressure (DBP) through miRNAs expression.

PATHWAY ANALYSIS FOR THE CANDIDATE miRNAs

The candidate miRNAs were subjected to pathway exploration using the Ingenuity Pathway Analysis (IPA) software (Ingenuity Systems, Redwood City, CA) .

Using this software, top-ranked pathways were also determined.

Moreover are provided the biological functions associated with these miRNAs, such as the diseases in which they are involved (Figure 22).



© 2000-2014 QIAGEN. All rights reserved.

Figure 22. Biological functions and diseases associated with candidate miRNAs

DISCUSSION

The purpose of this study was to investigate the changes in extracellular vesicles induced by PM₁₀ exposure both by observing changes in the number of specific subpopulations and quantifying the expression levels of miRNAs they contains. In the first part of the study, we analyzed the variation, in term of concentration, of plasma microvesicles in association with PM₁₀ exposure.

The choice of a population of overweight/obese individuals is justified by extensive scientific evidence that prove a link between obesity and air pollution; In fact, subjects with a greater body mass index seem to be more susceptible to the effect of acute inflammation triggered by exposure to PM₁₀, probably due to a greater absorption of the metals contained in it [93, 100] .

Hence, the obese population seems to represent a good population to investigate the effects of exposure to PM₁₀ in clinical and molecular level, as the most sensitive but healthy population.

In particular, for the study of MVs subpopulations, we decided to investigate 5 subpopulations of MVs by flow cytometry: MVs from monocytes (CD14+), MVs from platelets (CD61+), MVs from neutrophils (CD66+), MVs from endothelium (CD105+), MVs from epithelium (EpCAM+). We performed multiparametric analysis, evaluating multiple characteristics of the MVs as the integrity and the tissue of origin, through the use of antibodies specific for antigens of surface.

We focused on subpopulations of MVs involved in inflammation, coagulation and activation of pulmonary epithelial because we hypothesized that the increase of their concentration in plasma is associated with PM₁₀ exposure.

We assumed that PM₁₀ is able to establish a state of acute inflammation and damage at the level of the lung tissue and through the release of MVs can impact on the emergence of cardiovascular disease [101-103].

Plasma concentrations of MVs derived from platelets, monocytes, neutrophils and endothelial cells appear to be associated to PM₁₀ exposure, while the association was not significant for the lung epithelium-derived MVs. This could prove our assumption that basically is a cascade mechanisms of intercellular communication; starting by inflammation and activation of pulmonary epithelium, the MVs released could reach and activate the endothelial barrier and finally stimulate and determine the release of MVs by all hematopoietic cell types. For this reason they have not been found significant levels of MVs from lung epithelium in the plasma, as their major function would be performed at the interstitial level.

The total concentration of microvesicles was analyzed by NTA, allowing to separate the microvesicles by exosomes.

Microvesicles appear to be associated with exposure to PM₁₀, while the total amount of exosomes is not significant. This highlights the difference between the two types of vesicles, therefore exosomes and microvesicles may have a different role in the mechanisms of communication both pathological and physiological.

For miRNAs study, performed through TaqMan Open Array Real Time PCR, we test the association between PM₁₀ exposure and the different levels of expression of 733 human miRNAs (with known and unknown biological function).

This phase of the SPHERE study had the aim of screening the entire miRNome on a population of approximately 1000 subjects (half of the total population). In a second step the 52 miRNAs results as more associated with the PM₁₀ will be validated through standard Real Time- PCR on a population of comparable size.

Therefore, the data shown represent a first survey to which must necessarily follow a validation phase on selected miRNAs.

Finally, a standard approach was applied to perform mediation analysis in order to investigate the role of miRNAs expression as mediator of the effect of PM₁₀ on cardiac outcome: Systolic and Diastolic Blood Pressure. We applied Sobel test to test the null hypothesis that the “true” indirect effect is zero, with the p-value derived from the standard normal distribution. In particular, we can estimate that 36.8% of the effect of PM₁₀ on Systolic Blood Pressure is mediated by miR-106a.

Focusing on a preliminary analysis of miRNA-106a and through a literature review, has emerged an important role of this miRNA: modulating hematopoietic lineage determination and formation, including monocytopoiesis[104, 105].

Previous studies [106, 107] suggest that miR-106a (together with miR-17 and miR-20a) effectively regulate macrophage inflammatory responses through modulating leukocyte SIRPα synthesis. As an important signaling molecule, SIRPα modulates many aspects of leukocyte inflammatory responses, including activation, chemotaxis, and phagocytosis. miR-106a is involved in macrophage infiltration through the direct suppression of expression of signal-

regulatory protein α (SIRP α). A downregulation of mir-106a seems to act in favor of the differentiation of monocytes into macrophages as we can see in the Figure 23.

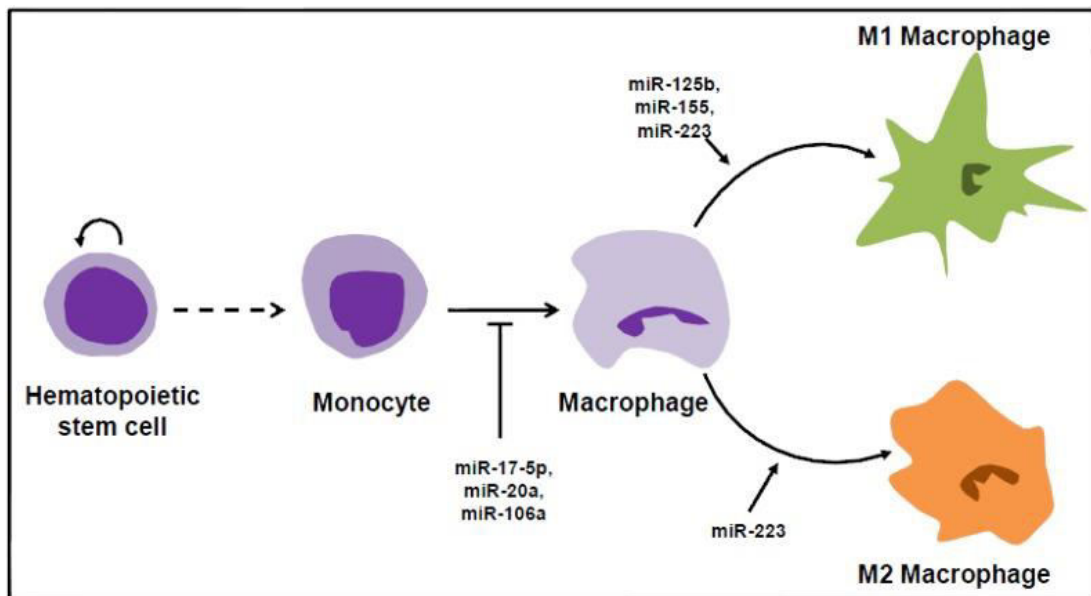


Figure 23. MicroRNA regulation of monocytic maturation and macrophage polarization. Chang, R.C., et al., *Cells*, 2014. **3**(3): p. 702-12.

Macrophage infiltration occurs in many tissue types, such as adipose tissue, the vascular system, liver and muscle and it is involved in the processes of formation of atherosclerotic plaques. The resident macrophages in tissues and organs play critical roles in controlling physiological functions and systemic homeostasis in tissues. miRNAs are a set of potent regulators of macrophage differentiation, infiltration, activation and cell-cell interactions.

Further investigations are required. In particular, after the validation phase will follow an investigation step using bioinformatics tools to clarify the role of identified miRNAs and their implications in biological processes and human diseases.

Future directions in research activities will be also to evaluate other exposure models: we will perform personal air pollution measures of PM, using passive samplers, on a subgroup of 200 selected subjects, and additionally will also be used metals determination in urine and hair to estimate short/medium term exposure.

The proposed research will help to shed light on the chain of events that from air pollution exposure leads to CVD trying to explore a new mechanism which involves alteration of extracellular vesicles production and content. Our findings, if confirmed, could lead to the identification of potentially-reversible alterations that might be also considered as potential target for new diagnostic and therapeutic interventions.

REFERENCES

1. (EPA), U.S.E.P.A., *Air Quality Criteria for Particulate Matter*, 2004.
2. Organization, W.H., *health effects of particulate matter*, 2013.
3. Europe, W.R.O.f., *Air quality guidelines: global update 2005. Particulate matter, ozone, nitrogen dioxide and sulfur dioxide*, 2006.
4. Samoli, E., et al., *Acute effects of ambient particulate matter on mortality in Europe and North America: results from the APHENA study*. *Environ Health Perspect*, 2008. **116**(11): p. 1480-6.
5. Beelen, R., et al., *Long-term effects of traffic-related air pollution on mortality in a Dutch cohort (NLCS-AIR study)*. *Environ Health Perspect*, 2008. **116**(2): p. 196-202.
6. Krewski, D., et al., *Extended follow-up and spatial analysis of the American Cancer Society study linking particulate air pollution and mortality*. *Res Rep Health Eff Inst*, 2009(140): p. 5-114; discussion 115-36.
7. Pope, C.A., 3rd, et al., *Lung cancer, cardiopulmonary mortality, and long-term exposure to fine particulate air pollution*. *JAMA*, 2002. **287**(9): p. 1132-41.
8. Europe, W.R.O.f., *Exposure to air pollution (particulate matter) in outdoor air*, 2011.
9. Europe, W.R.O.f., *Health relevance of particulate matter from various sources*, 2007.
10. Pope, C.A., 3rd, et al., *Particulate air pollution as a predictor of mortality in a prospective study of U.S. adults*. *Am J Respir Crit Care Med*, 1995. **151**(3 Pt 1): p. 669-74.
11. Dockery, D.W., et al., *An association between air pollution and mortality in six U.S. cities*. *N Engl J Med*, 1993. **329**(24): p. 1753-9.
12. Samet, J.M., et al., *Fine particulate air pollution and mortality in 20 U.S. cities, 1987-1994*. *N Engl J Med*, 2000. **343**(24): p. 1742-9.
13. Brook, R.D., et al., *Particulate matter air pollution and cardiovascular disease: An update to the scientific statement from the American Heart Association*. *Circulation*, 2010. **121**(21): p. 2331-78.
14. Chen, L.C. and J.S. Hwang, *Effects of subchronic exposures to concentrated ambient particles (CAPs) in mice. IV. Characterization of acute and chronic effects of ambient air fine particulate matter exposures on heart-rate variability*. *Inhal Toxicol*, 2005. **17**(4-5): p. 209-16.
15. Sun, Q., et al., *Long-term air pollution exposure and acceleration of atherosclerosis and vascular inflammation in an animal model*. *JAMA*, 2005. **294**(23): p. 3003-10.
16. Ridker, P.M., et al., *Prospective study of herpes simplex virus, cytomegalovirus, and the risk of future myocardial infarction and stroke*. *Circulation*, 1998. **98**(25): p. 2796-9.
17. Wennberg, P., et al., *Haemostatic and inflammatory markers are independently associated with myocardial infarction in men and women*. *Thromb Res*, 2012. **129**(1): p. 68-73.
18. Ruckerl, R., et al., *Air pollution and markers of inflammation and coagulation in patients with coronary heart disease*. *Am J Respir Crit Care Med*, 2006. **173**(4): p. 432-41.
19. Hoffmann, B., et al., *Chronic residential exposure to particulate matter air pollution and systemic inflammatory markers*. *Environ Health Perspect*, 2009. **117**(8): p. 1302-8.

20. Chuang, K.J., et al., *The effect of urban air pollution on inflammation, oxidative stress, coagulation, and autonomic dysfunction in young adults*. Am J Respir Crit Care Med, 2007. **176**(4): p. 370-6.
21. Schicker, B., et al., *Particulate matter inhalation during hay storing activity induces systemic inflammation and platelet aggregation*. Eur J Appl Physiol, 2009. **105**(5): p. 771-8.
22. Nemmar, A., et al., *Diesel exhaust particles in lung acutely enhance experimental peripheral thrombosis*. Circulation, 2003. **107**(8): p. 1202-8.
23. Hristov, M., et al., *Apoptotic bodies from endothelial cells enhance the number and initiate the differentiation of human endothelial progenitor cells in vitro*. Blood, 2004. **104**(9): p. 2761-6.
24. Trams, E.G., et al., *Exfoliation of membrane ecto-enzymes in the form of microvesicles*. Biochim Biophys Acta, 1981. **645**(1): p. 63-70.
25. Harding, C., J. Heuser, and P. Stahl, *Endocytosis and intracellular processing of transferrin and colloidal gold-transferrin in rat reticulocytes: demonstration of a pathway for receptor shedding*. Eur J Cell Biol, 1984. **35**(2): p. 256-63.
26. Mathivanan, S., H. Ji, and R.J. Simpson, *Exosomes: extracellular organelles important in intercellular communication*. J Proteomics, 2010. **73**(10): p. 1907-20.
27. Sullivan, R., et al., *Role of exosomes in sperm maturation during the transit along the male reproductive tract*. Blood Cells Mol Dis, 2005. **35**(1): p. 1-10.
28. Pisitkun, T., R.F. Shen, and M.A. Knepper, *Identification and proteomic profiling of exosomes in human urine*. Proc Natl Acad Sci U S A, 2004. **101**(36): p. 13368-73.
29. Caby, M.P., et al., *Exosomal-like vesicles are present in human blood plasma*. Int Immunol, 2005. **17**(7): p. 879-87.
30. Admyre, C., et al., *Exosomes with major histocompatibility complex class II and costimulatory molecules are present in human BAL fluid*. Eur Respir J, 2003. **22**(4): p. 578-83.
31. Revenfeld, A.L., et al., *Diagnostic and Prognostic Potential of Extracellular Vesicles in Peripheral Blood*. Clin Ther, 2014. **36**(6): p. 830-846.
32. Mathivanan, S. and R.J. Simpson, *ExoCarta: A compendium of exosomal proteins and RNA*. Proteomics, 2009. **9**(21): p. 4997-5000.
33. Palay, S.L., *The fine structure of secretory neurons in the preoptic nucleus of the goldfish (Carassius auratus)*. Anat Rec, 1960. **138**: p. 417-43.
34. Roizin, L., et al., *The fine structure of the multivesicular body and their relationship to the ultracellular constituents of the central nervous system*. J Neuropathol Exp Neurol, 1967. **26**(2): p. 223-49.
35. Babst, M., et al., *Escrt-III: an endosome-associated heterooligomeric protein complex required for mvb sorting*. Dev Cell, 2002. **3**(2): p. 271-82.
36. Wollert, T. and J.H. Hurley, *Molecular mechanism of multivesicular body biogenesis by ESCRT complexes*. Nature, 2010. **464**(7290): p. 864-9.
37. Borges, F.T., et al., *TGF-beta1-containing exosomes from injured epithelial cells activate fibroblasts to initiate tissue regenerative responses and fibrosis*. J Am Soc Nephrol, 2013. **24**(3): p. 385-92.
38. D'Souza-Schorey, C. and J.W. Clancy, *Tumor-derived microvesicles: shedding light on novel microenvironment modulators and prospective cancer biomarkers*. Genes Dev, 2012. **26**(12): p. 1287-99.
39. Skog, J., et al., *Glioblastoma microvesicles transport RNA and proteins that promote tumour growth and provide diagnostic biomarkers*. Nat Cell Biol, 2008. **10**(12): p. 1470-6.

40. Morel, O., et al., *Cellular mechanisms underlying the formation of circulating microparticles*. *Arterioscler Thromb Vasc Biol*, 2011. **31**(1): p. 15-26.
41. Raiborg, C. and H. Stenmark, *The ESCRT machinery in endosomal sorting of ubiquitylated membrane proteins*. *Nature*, 2009. **458**(7237): p. 445-52.
42. Baietti, M.F., et al., *Syndecan-syntenin-ALIX regulates the biogenesis of exosomes*. *Nat Cell Biol*, 2012. **14**(7): p. 677-85.
43. Nabhan, J.F., et al., *Formation and release of arrestin domain-containing protein 1-mediated microvesicles (ARMMs) at plasma membrane by recruitment of TSG101 protein*. *Proc Natl Acad Sci U S A*, 2012. **109**(11): p. 4146-51.
44. Muralidharan-Chari, V., et al., *ARF6-regulated shedding of tumor cell-derived plasma membrane microvesicles*. *Curr Biol*, 2009. **19**(22): p. 1875-85.
45. S, E.L.A., et al., *Extracellular vesicles: biology and emerging therapeutic opportunities*. *Nat Rev Drug Discov*, 2013. **12**(5): p. 347-57.
46. Zhang, B., et al., *microRNAs as oncogenes and tumor suppressors*. *Dev Biol*, 2007. **302**(1): p. 1-12.
47. Jackson, R.J. and N. Standart, *How do microRNAs regulate gene expression?* *Sci STKE*, 2007. **2007**(367): p. re1.
48. Nilsen, T.W., *Mechanisms of microRNA-mediated gene regulation in animal cells*. *Trends Genet*, 2007. **23**(5): p. 243-9.
49. Castanotto, D., et al., *Short hairpin RNA-directed cytosine (CpG) methylation of the RASSF1A gene promoter in HeLa cells*. *Mol Ther*, 2005. **12**(1): p. 179-83.
50. He, L. and G.J. Hannon, *MicroRNAs: small RNAs with a big role in gene regulation*. *Nat Rev Genet*, 2004. **5**(7): p. 522-31.
51. Janowska-Wieczorek, A., et al., *Platelet-derived microparticles bind to hematopoietic stem/progenitor cells and enhance their engraftment*. *Blood*, 2001. **98**(10): p. 3143-9.
52. Camussi, G., et al., *Exosomes/microvesicles as a mechanism of cell-to-cell communication*. *Kidney Int*, 2010. **78**(9): p. 838-48.
53. Losche, W., et al., *Platelet-derived microvesicles transfer tissue factor to monocytes but not to neutrophils*. *Platelets*, 2004. **15**(2): p. 109-15.
54. Lee, Y., S. El Andaloussi, and M.J. Wood, *Exosomes and microvesicles: extracellular vesicles for genetic information transfer and gene therapy*. *Hum Mol Genet*, 2012. **21**(R1): p. R125-34.
55. Camussi, G., et al., *Exosome/microvesicle-mediated epigenetic reprogramming of cells*. *Am J Cancer Res*, 2011. **1**(1): p. 98-110.
56. Cocucci, E., G. Racchetti, and J. Meldolesi, *Shedding microvesicles: artefacts no more*. *Trends Cell Biol*, 2009. **19**(2): p. 43-51.
57. Ratajczak, J., et al., *Embryonic stem cell-derived microvesicles reprogram hematopoietic progenitors: evidence for horizontal transfer of mRNA and protein delivery*. *Leukemia*, 2006. **20**(5): p. 847-56.
58. Gatti, S., et al., *Microvesicles derived from human adult mesenchymal stem cells protect against ischaemia-reperfusion-induced acute and chronic kidney injury*. *Nephrol Dial Transplant*, 2011. **26**(5): p. 1474-83.
59. Raposo, G., et al., *B lymphocytes secrete antigen-presenting vesicles*. *J Exp Med*, 1996. **183**(3): p. 1161-72.
60. Del Conde, I., et al., *Tissue-factor-bearing microvesicles arise from lipid rafts and fuse with activated platelets to initiate coagulation*. *Blood*, 2005. **106**(5): p. 1604-11.
61. Clayton, A., et al., *Human tumor-derived exosomes selectively impair lymphocyte responses to interleukin-2*. *Cancer Res*, 2007. **67**(15): p. 7458-66.
62. Clayton, A., et al., *Human tumor-derived exosomes down-modulate NKG2D expression*. *J Immunol*, 2008. **180**(11): p. 7249-58.

63. Yu, S., et al., *Tumor exosomes inhibit differentiation of bone marrow dendritic cells*. J Immunol, 2007. **178**(11): p. 6867-75.
64. Baj-Krzyworzeka, M., et al., *Tumour-derived microvesicles modulate biological activity of human monocytes*. Immunol Lett, 2007. **113**(2): p. 76-82.
65. Sprague, D.L., et al., *Platelet-mediated modulation of adaptive immunity: unique delivery of CD154 signal by platelet-derived membrane vesicles*. Blood, 2008. **111**(10): p. 5028-36.
66. Simhadri, V.R., et al., *Dendritic cells release HLA-B-associated transcript-3 positive exosomes to regulate natural killer function*. PLoS One, 2008. **3**(10): p. e3377.
67. Lachenal, G., et al., *Release of exosomes from differentiated neurons and its regulation by synaptic glutamatergic activity*. Mol Cell Neurosci, 2011. **46**(2): p. 409-18.
68. Aliotta, J.M., et al., *Alteration of marrow cell gene expression, protein production, and engraftment into lung by lung-derived microvesicles: a novel mechanism for phenotype modulation*. Stem Cells, 2007. **25**(9): p. 2245-56.
69. Rak, J. and A. Guha, *Extracellular vesicles--vehicles that spread cancer genes*. Bioessays, 2012. **34**(6): p. 489-97.
70. Al-Nedawi, K., et al., *Intercellular transfer of the oncogenic receptor EGFRvIII by microvesicles derived from tumour cells*. Nat Cell Biol, 2008. **10**(5): p. 619-24.
71. Al-Nedawi, K., et al., *Endothelial expression of autocrine VEGF upon the uptake of tumor-derived microvesicles containing oncogenic EGFR*. Proc Natl Acad Sci U S A, 2009. **106**(10): p. 3794-9.
72. Sidhu, S.S., et al., *The microvesicle as a vehicle for EMMPRIN in tumor-stromal interactions*. Oncogene, 2004. **23**(4): p. 956-63.
73. Wieckowski, E.U., et al., *Tumor-derived microvesicles promote regulatory T cell expansion and induce apoptosis in tumor-reactive activated CD8+ T lymphocytes*. J Immunol, 2009. **183**(6): p. 3720-30.
74. Kim, J.W., et al., *Fas ligand-positive membranous vesicles isolated from sera of patients with oral cancer induce apoptosis of activated T lymphocytes*. Clin Cancer Res, 2005. **11**(3): p. 1010-20.
75. Mack, M., et al., *Transfer of the chemokine receptor CCR5 between cells by membrane-derived microparticles: a mechanism for cellular human immunodeficiency virus 1 infection*. Nat Med, 2000. **6**(7): p. 769-75.
76. Pegtel, D.M., et al., *Functional delivery of viral miRNAs via exosomes*. Proc Natl Acad Sci U S A, 2010. **107**(14): p. 6328-33.
77. Chivet, M., et al., *Emerging role of neuronal exosomes in the central nervous system*. Front Physiol, 2012. **3**: p. 145.
78. Bellingham, S.A., et al., *Exosomes: vehicles for the transfer of toxic proteins associated with neurodegenerative diseases? Front Physiol, 2012. **3**: p. 124.*
79. Emmanouilidou, E., et al., *Cell-produced alpha-synuclein is secreted in a calcium-dependent manner by exosomes and impacts neuronal survival*. J Neurosci, 2010. **30**(20): p. 6838-51.
80. Levanen, B., et al., *Altered microRNA profiles in bronchoalveolar lavage fluid exosomes in asthmatic patients*. J Allergy Clin Immunol, 2013. **131**(3): p. 894-903.
81. Kuwabara, Y., et al., *Increased microRNA-1 and microRNA-133a levels in serum of patients with cardiovascular disease indicate myocardial damage*. Circ Cardiovasc Genet, 2011. **4**(4): p. 446-54.
82. Gildea, J.J., et al., *Urinary exosome miRNome analysis and its applications to salt sensitivity of blood pressure*. Clin Biochem, 2013. **46**(12): p. 1131-4.

83. Zhang, Y., et al., *Secreted monocytic miR-150 enhances targeted endothelial cell migration*. Mol Cell, 2010. **39**(1): p. 133-44.
84. Ogata-Kawata, H., et al., *Circulating exosomal microRNAs as biomarkers of colon cancer*. Plos One, 2014. **9**(4): p. e92921.
85. Yamada, N., et al., *Role of Intracellular and Extracellular MicroRNA-92a in Colorectal Cancer*. Transl Oncol, 2013. **6**(4): p. 482-92.
86. Silva, J., et al., *Vesicle-related microRNAs in plasma of nonsmall cell lung cancer patients and correlation with survival*. Eur Respir J, 2011. **37**(3): p. 617-23.
87. Aushev, V.N., et al., *Comparisons of microRNA patterns in plasma before and after tumor removal reveal new biomarkers of lung squamous cell carcinoma*. Plos One, 2013. **8**(10): p. e78649.
88. Tadokoro, H., et al., *Exosomes derived from hypoxic leukemia cells enhance tube formation in endothelial cells*. J Biol Chem, 2013. **288**(48): p. 34343-51.
89. Camacho, L., P. Guerrero, and D. Marchetti, *MicroRNA and protein profiling of brain metastasis competent cell-derived exosomes*. PLoS One, 2013. **8**(9): p. e73790.
90. Rana, S., K. Malinowska, and M. Zoller, *Exosomal tumor microRNA modulates premetastatic organ cells*. Neoplasia, 2013. **15**(3): p. 281-95.
91. Xin, M., E.N. Olson, and R. Bassel-Duby, *Mending broken hearts: cardiac development as a basis for adult heart regeneration and repair*. Nat Rev Mol Cell Biol, 2013. **14**(8): p. 529-41.
92. Hergenreider, E., et al., *Atheroprotective communication between endothelial cells and smooth muscle cells through miRNAs*. Nat Cell Biol, 2012. **14**(3): p. 249-56.
93. Zhao, Y., et al., *Does obesity amplify the association between ambient air pollution and increased blood pressure and hypertension in adults? Findings from the 33 Communities Chinese Health Study*. Int J Cardiol, 2013. **168**(5): p. e148-50.
94. Bernal-Mizrachi, L., et al., *Endothelial microparticles correlate with high-risk angiographic lesions in acute coronary syndromes*. Int J Cardiol, 2004. **97**(3): p. 439-46.
95. Dubowsky, S.D., et al., *Diabetes, obesity, and hypertension may enhance associations between air pollution and markers of systemic inflammation*. Environ Health Perspect, 2006. **114**(7): p. 992-8.
96. Moore, M.L., C. Engwall, and P.A. Moskal, *Methodology of Isolation, Identification and Incidence of Clostridia from Clinical Material*. Am J Med Technol, 1964. **30**: p. 385-7.
97. Liu, M.L., et al., *Cholesterol enrichment of human monocyte/macrophages induces surface exposure of phosphatidylserine and the release of biologically-active tissue factor-positive microvesicles*. Arterioscler Thromb Vasc Biol, 2007. **27**(2): p. 430-5.
98. Taylor, D.D. and C. Gercel-Taylor, *MicroRNA signatures of tumor-derived exosomes as diagnostic biomarkers of ovarian cancer*. Gynecol Oncol, 2008. **110**(1): p. 13-21.
99. Dragovic, R.A., et al., *Sizing and phenotyping of cellular vesicles using Nanoparticle Tracking Analysis*. Nanomedicine, 2011. **7**(6): p. 780-8.
100. Curtis, A.M., et al., *Endothelial microparticles: sophisticated vesicles modulating vascular function*. Vasc Med, 2013. **18**(4): p. 204-14.
101. Pope, C.A., 3rd, *Mortality effects of longer term exposures to fine particulate air pollution: review of recent epidemiological evidence*. Inhal Toxicol, 2007. **19 Suppl 1**: p. 33-8.
102. Corey, L.M., C. Baker, and D.L. Luchtel, *Heart-rate variability in the apolipoprotein E knockout transgenic mouse following exposure to Seattle particulate matter*. J Toxicol Environ Health A, 2006. **69**(10): p. 953-65.

103. Jy, W., et al., *Measuring circulating cell-derived microparticles*. J Thromb Haemost, 2004. **2**(10): p. 1842-51.
104. Chen, C.Z., et al., *MicroRNAs modulate hematopoietic lineage differentiation*. Science, 2004. **303**(5654): p. 83-6.
105. Monticelli, S., et al., *MicroRNA profiling of the murine hematopoietic system*. Genome Biol, 2005. **6**(8): p. R71.
106. Zhu, D., et al., *MicroRNA-17/20a/106a modulate macrophage inflammatory responses through targeting signal-regulatory protein alpha*. J Allergy Clin Immunol, 2013. **132**(2): p. 426-36 e8.
107. Chang, R.C., et al., *MicroRNAs Control Macrophage Formation and Activation: The Inflammatory Link between Obesity and Cardiovascular Diseases*. Cells, 2014. **3**(3): p. 702-12.